Electronic Supplementary Information

Table of contents

1. Studies on the conversion of benzoquinolizinium 3b to benzothiophene 6

1.1 Conversion of 3b to 6 in DMSO-d_6

A solution of **3b** (3.5 mg) in DMSO-d_6 (600 µL) was monitored by ^{1}H-NMR spectroscopy by recording a spectrum every 10 min for 5 h (Figure S1). The conversion was analyzed with a plot of the change of the integrals of protons 6-H (**3b**, 10.70 ppm) and 7-H (**6**, 7.63 ppm) versus time (Figure S2). The resulting product was identified as the 2-benzo[*c*]thiophen-4-ylmethyl pyridine (**7**). ^{1}H-NMR (500 MHz, DMSO-d_6): δ = 4.64 (s, 2H, CH_2), 6.92 (dd, ^3J = 7 Hz, ^4J = 1 Hz, 1H, 5-H), 7.05 (dd, ^3J = 9 Hz, ^3J = 7 Hz, 1H, 6-H), 7.63 (d, ^3J = 9 Hz, 1H, 7-H), 7.78 (d, ^3J = 8.0 Hz, 1H, 3'-H), 7.82 (t, ^3J = 7 Hz, 1H, 5'-H), 8.08 (s, 2H, 1-H, 3-H), 8.35 (t, ^3J = 8 Hz, 1H, 4'-H), 8.81–8.84 (m, 1H, 6'-H). – ^{13}C-NMR: (150 MHz, DMSO-d_6): δ = 37.2 (CH_2), 116.3 (C3), 119.1 (C1), 121.7 (C7), 123.4 (C6), 123.8 (C5), 124.6 (C5'), 126.7 (C3'), 129.0 (C4), 137.2 (C3a), 138.2 (C7a), 143.1 (C6'), 145.0 (C4'), 155.5 (C2').

1.2 Protonation of the free base of 6

To a solution of **6** derived from **3b** (3.2 mg) in DMSO-d_6 (600 µL) (see above) were added 2 molar equivalents of hydrobromic acid (aq. 48%) and an ^{1}H-NMR spectrum was recorded directly after addition of the acid and after 3 h of addition (Figure S8).

1.3 Conversion of 3b to 7 in D_2O

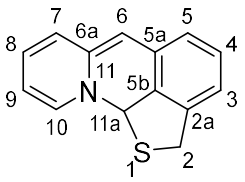

A mixture of **3b** (3.5 mg) in D_2O (600 µL) was suspended in an ultrasonic bath for 1 min until all components were dissolved. The resulting yellow solution was submitted to NMR-spectroscopic analysis (^{1}H-, ^{13}C-NMR, 1D-sel-TOCSY, TOCSY, COSY, HSQC, HMBC; Figure S9–13). The main compound (78%) present in the solution was identified as the 2,11a-dihydropyrido[1,2-*b*]thieno[4,3,2-*ij*]isoquinoline (**7**). ^{1}H-NMR (600 MHz, D_2O): δ = 4.52 (dd, ^4J = 14 Hz, ^5J = 3 Hz, 1H, 11a-H), 4.82 [d, ^4J = 14 Hz (determined from 1D sel. TOCSY), 2H, 2-H], 7.11 (d, ^5J = 3 Hz, 1H, 6-H), 7.41 (d, ^3J = 8 Hz, 1H, 3-H), 7.48 (d, ^3J = 7 Hz, 1H, 5-H), 7.54 (t, ^3J = 8 Hz, 1H, 4-H), 8.00 (t, ^3J = 7 Hz, 1H, 9-H), 8.14 (d, ^3J = 8 Hz, 1H, 7-H), 8.48 (t, ^3J = 8 Hz, 1H, 8-H), 9.21 (d, ^3J = 7 Hz, 1H, 10H). – ^{13}C-NMR (150 MHz, D_2O): δ = 42.8 (C11a, C2), 80.2 (C6), 126.8 (C3), 128.0 (C5), 128.4 (C9), 130.5 (C7), 133.1 (C5a), 133. 9 (C4), 137.9 (C5b), 140.9 (C2a), 144.6 (C10), 148.3 (C8), 156.5 (C6a).

Another ^{1}H-NMR spectrum was recorded after 2 d to investigate whether **7** is transformed to **6** (Figure S14). However, the spectrum indicated that **7** decomposed steadily over time.

1.4 Conversion of 3b to 6–D in CD_3OD

A solution of **3b** (2.6 mg) in CD_3OD (600 µL) was monitored by ^{1}H-NMR spectroscopy for 5 d (Figure S15). The resulting product was analyzed by ^{1}H- and ^{13}C-NMR and COSY, HSQC and HMBC experiments (Figures S16–20). The resulting product was identified as the 2-benzo[*c*]thiophen-4-ylmethyl pyridine (**6–D**). ^{1}H-NMR (500 MHz, CD_3OD): δ = 4.73 (s, 1H, CDH) 6.97 (dt, ^{3}J = 7 Hz, ^{4}J = 1 Hz, 1H, 5-H), 7.08 (dd, ^{3}J = 9 Hz, ^{3}J = 7 Hz, 1H, 6-H), 7.67 (d, ^{3}J = 9 Hz, 1H, 7-H), 7.80 (dd, ^{4}J = 3 Hz, ^{4}J = 1 Hz, 1H, 1-H), 7.90 (d, ^{3}J = 8 Hz, 1H, 3'-H), 7.94 (d, ^{4}J = 3 Hz, 1H, 3-H), 7.95–7.98 (m, 1H, 5'-H), 8.51 (td, ^{3}J = 8 Hz, ^{4}J = 2 Hz, 1H, 4'-H), 8.77 (ddd, ^{3}J = 6 Hz, ^{4}J = 2 Hz, ^{5}J = 1 Hz, 1H, 6'-H). – ^{13}C-NMR (150 MHz, CD_3OD): δ = 37.8 (CH_2–D_1), 116.2 (C1), 120.1 (C3), 123.6 (C7), 124.4 (C6), 125.9 (C5), 126.5 (C5'), 128.1 (C4), 129.0 (C3'), 138.7 (C3a), 140.2 (C7a), 142.7 (C6'), 148.3 (C4'), 156.9 (C2').

1.5 Stability of 6 in acidic buffer solution

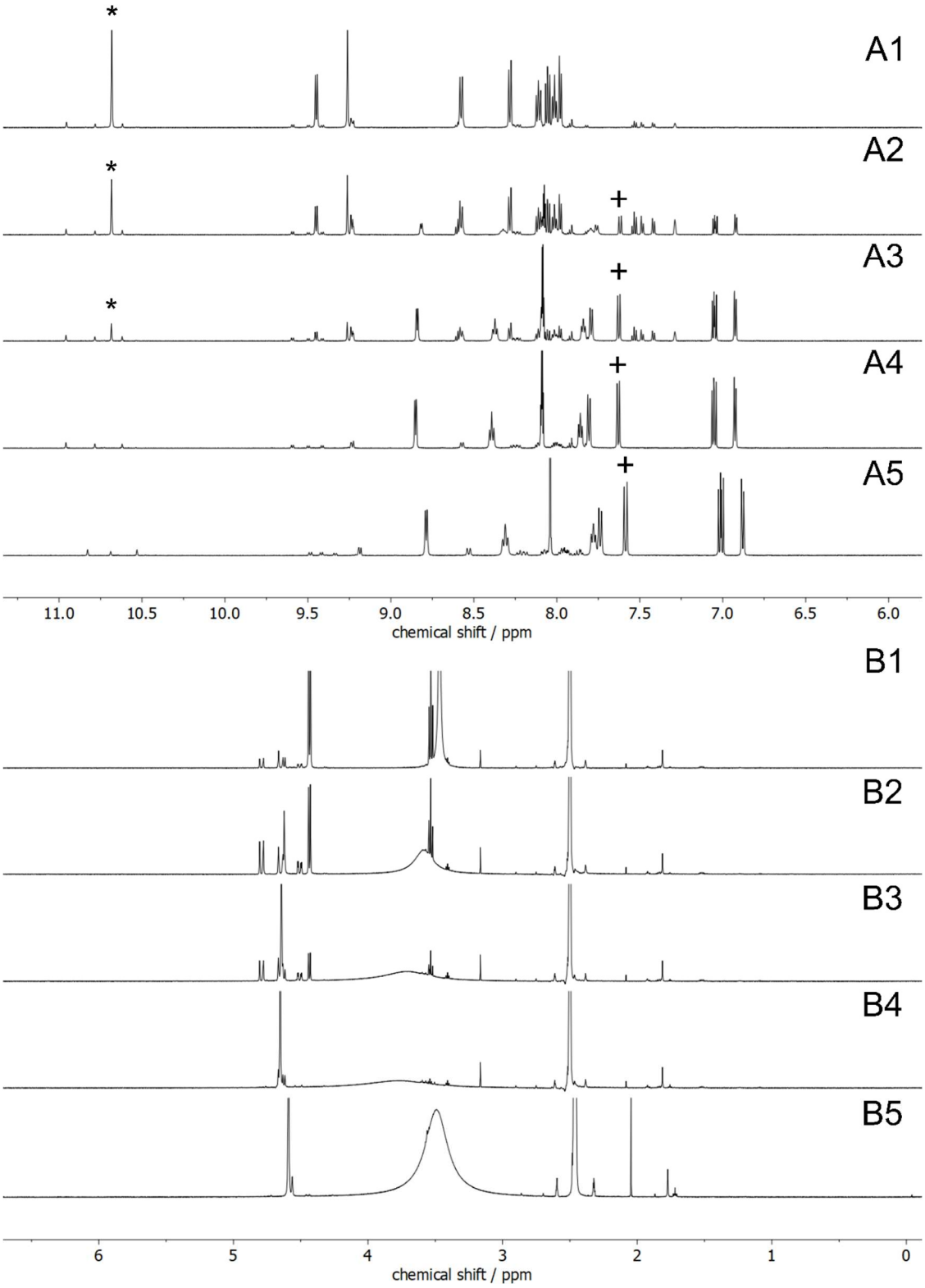

Figure S1. ^{1}H-NMR spectrum (600 MHz, 25 °C) of **3b** in DMSO-d_6 (6–11 ppm, A; 0–6 ppm, B) after 3 min (1), 33 min (2), 73 min (3), 293 min (4), and 3 d (5). ✶: Characteristic signal of **3b**; **+**: Characteristic signal of **6**.

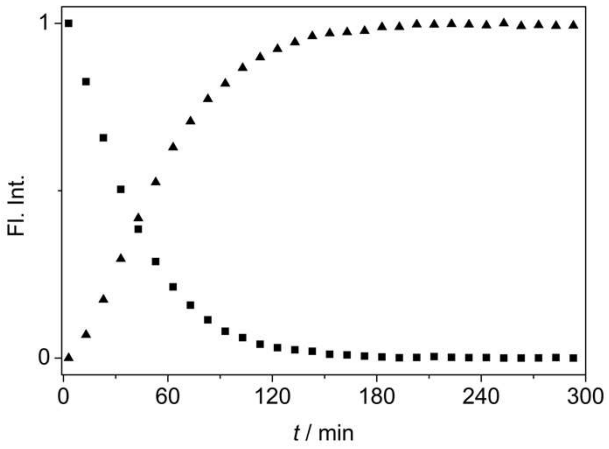

Figure S2. Change of the integrals of the ^{1}H-NMR signals of 6-H of **3b** (10.70 ppm, squares) and 7-H of **7** (7.63 ppm triangles) with time during conversion of **3b** to **6** in DMSO-d_6.

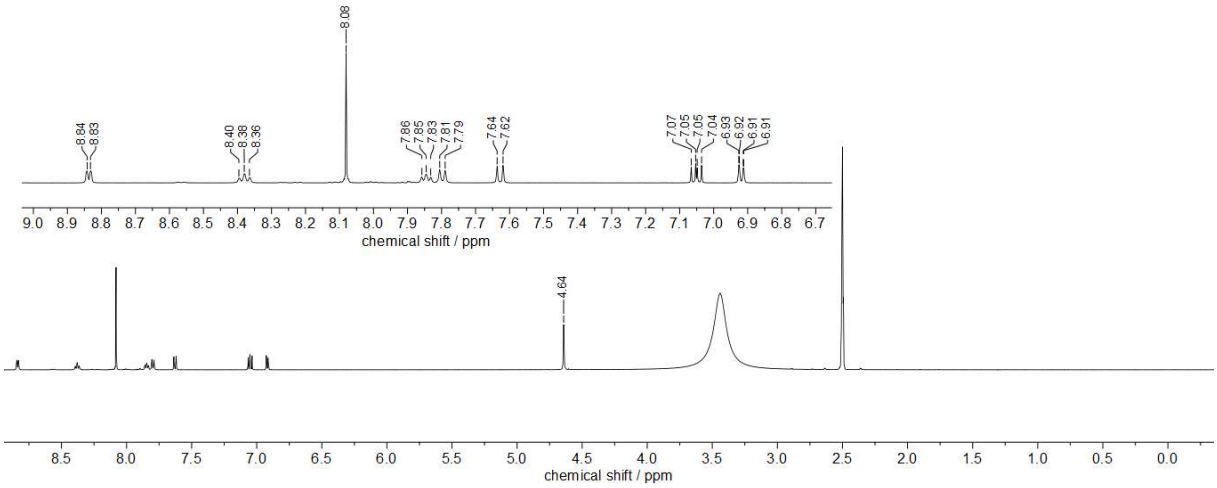

Figure S3. ^{1}H-NMR spectrum (500 MHz, DMSO-d_6, 25 °C) of **6** derived from **3b**.

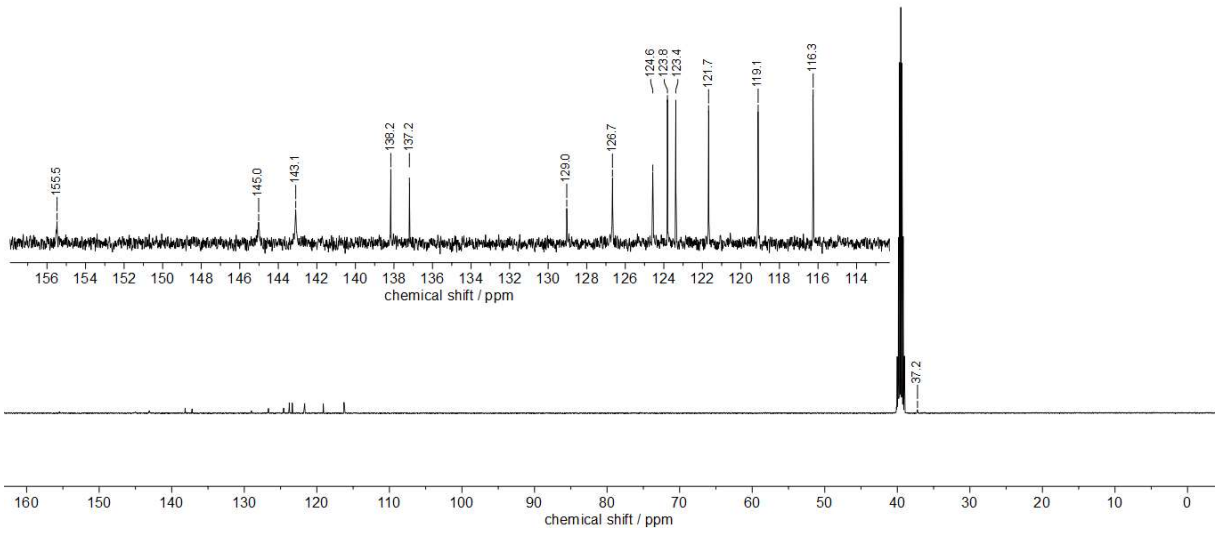

Figure S4. ^{13}C-NMR spectrum (125 MHz, DMSO-d_6, 25 °C) of **6** derived from **3b**.

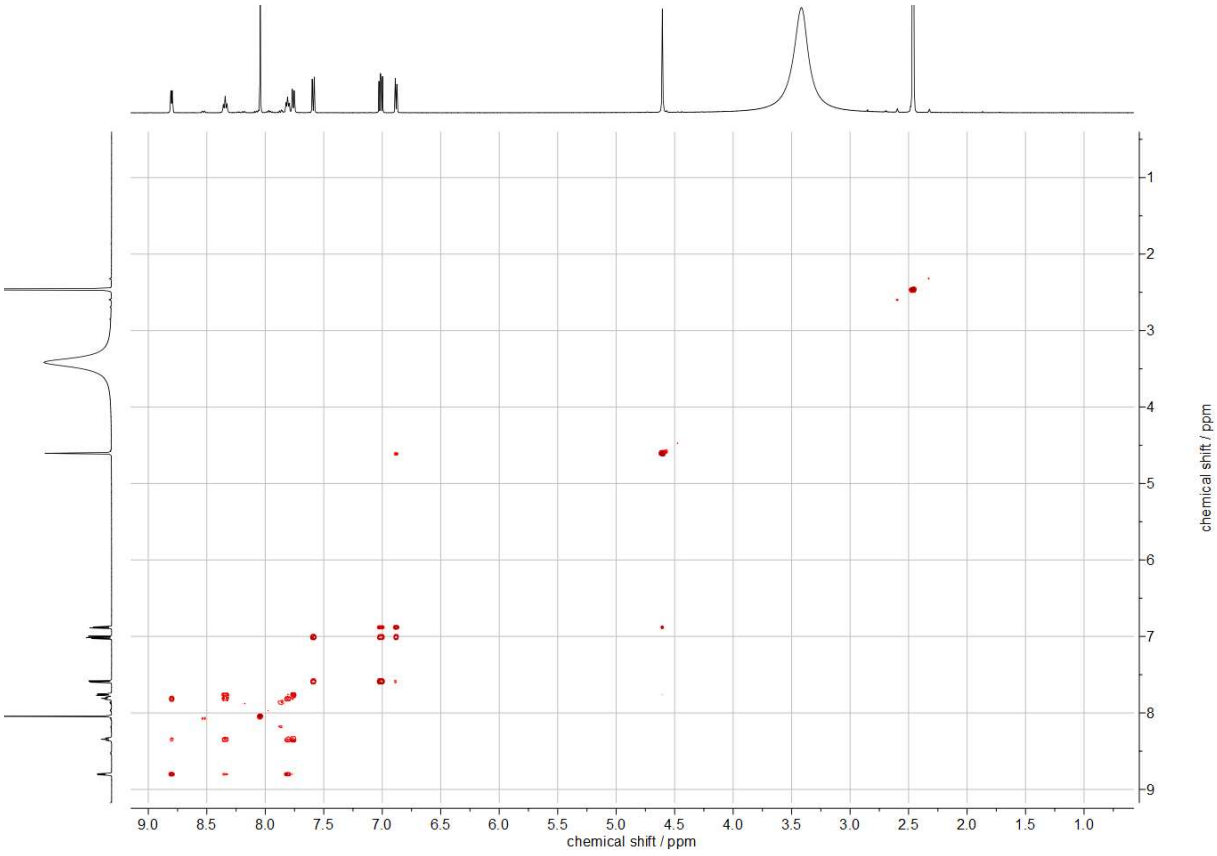

Figure S5. HH-COSY spectrum (500 MHz, DMSO-d_6, 25 °C) of **6** derived from **3b**.

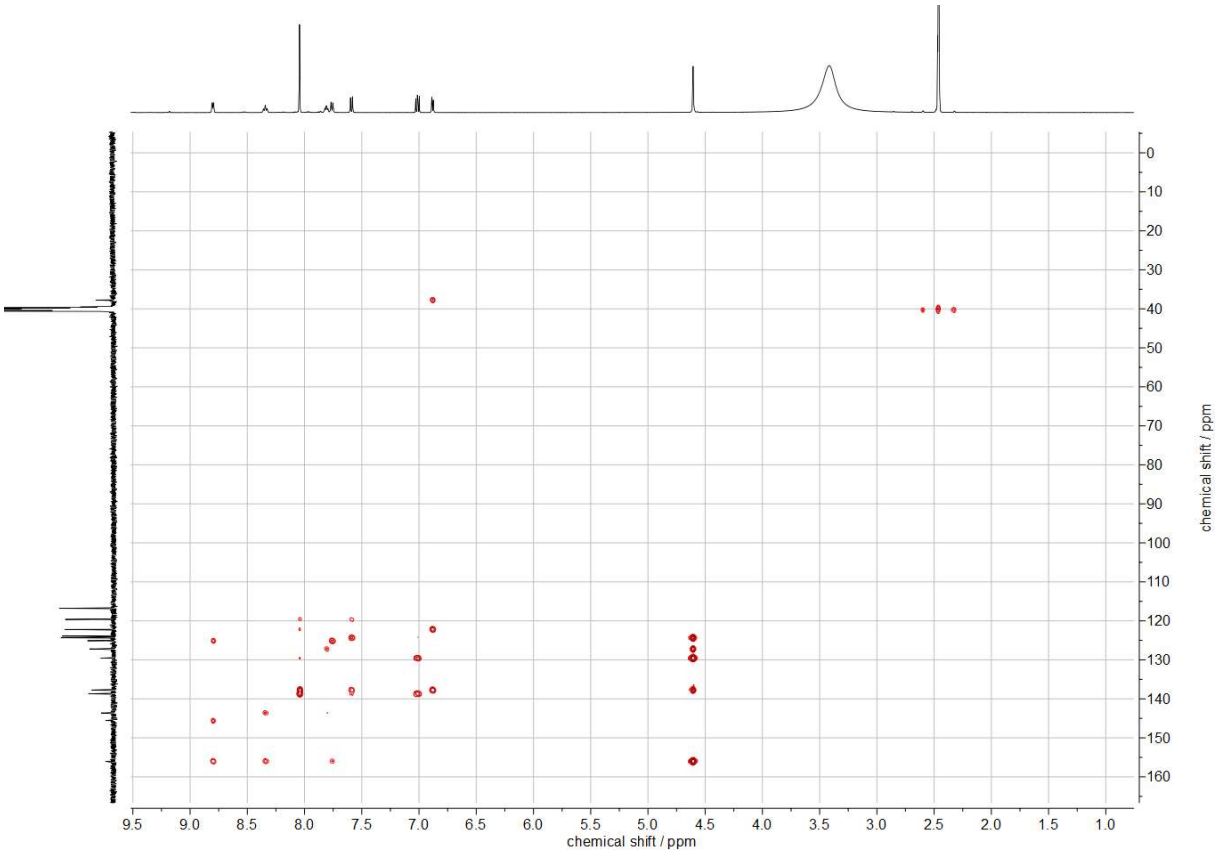

Figure S6. HSQC spectrum (600 MHz, DMSO-d_6, 25 °C) of **6** derived from **3b**.

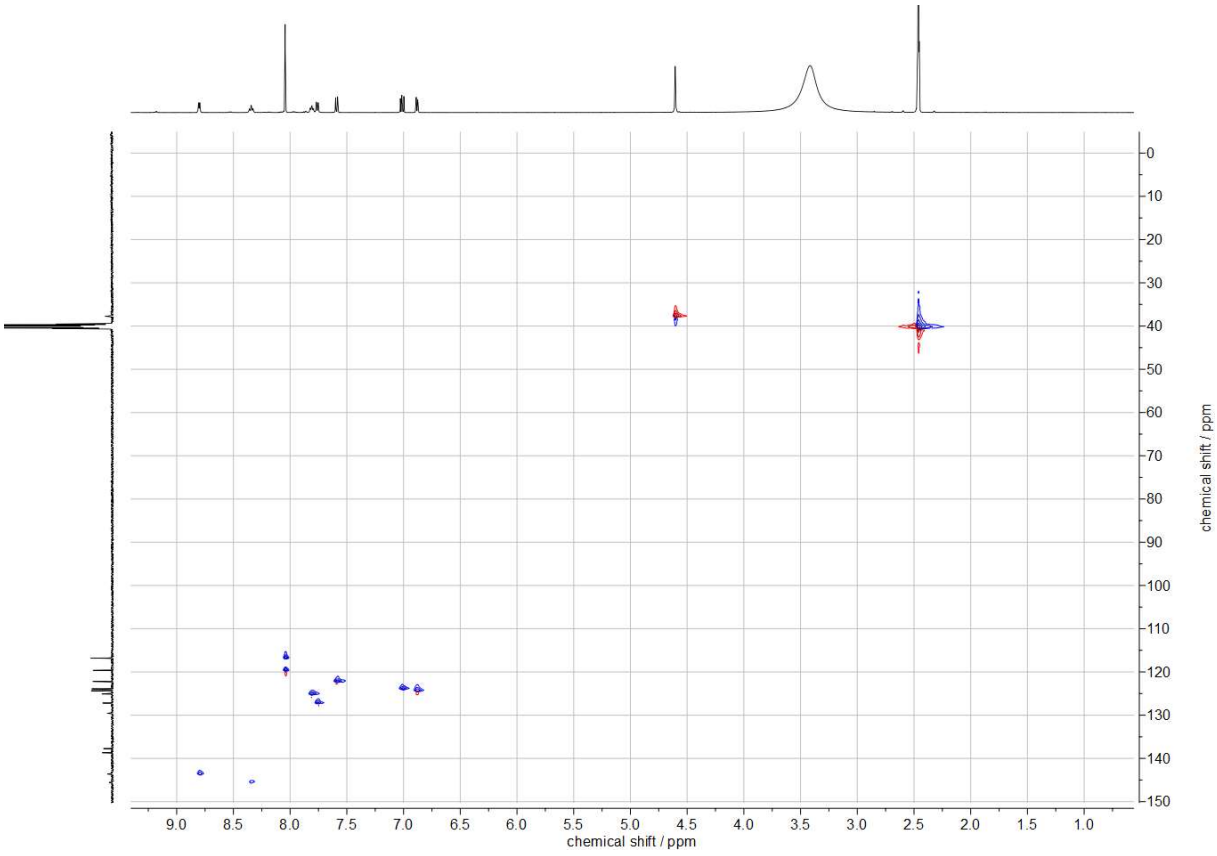

Figure S7. HMBC spectrum (500 MHz, DMSO-d_6, 25 °C) of **6** derived from **3b**.

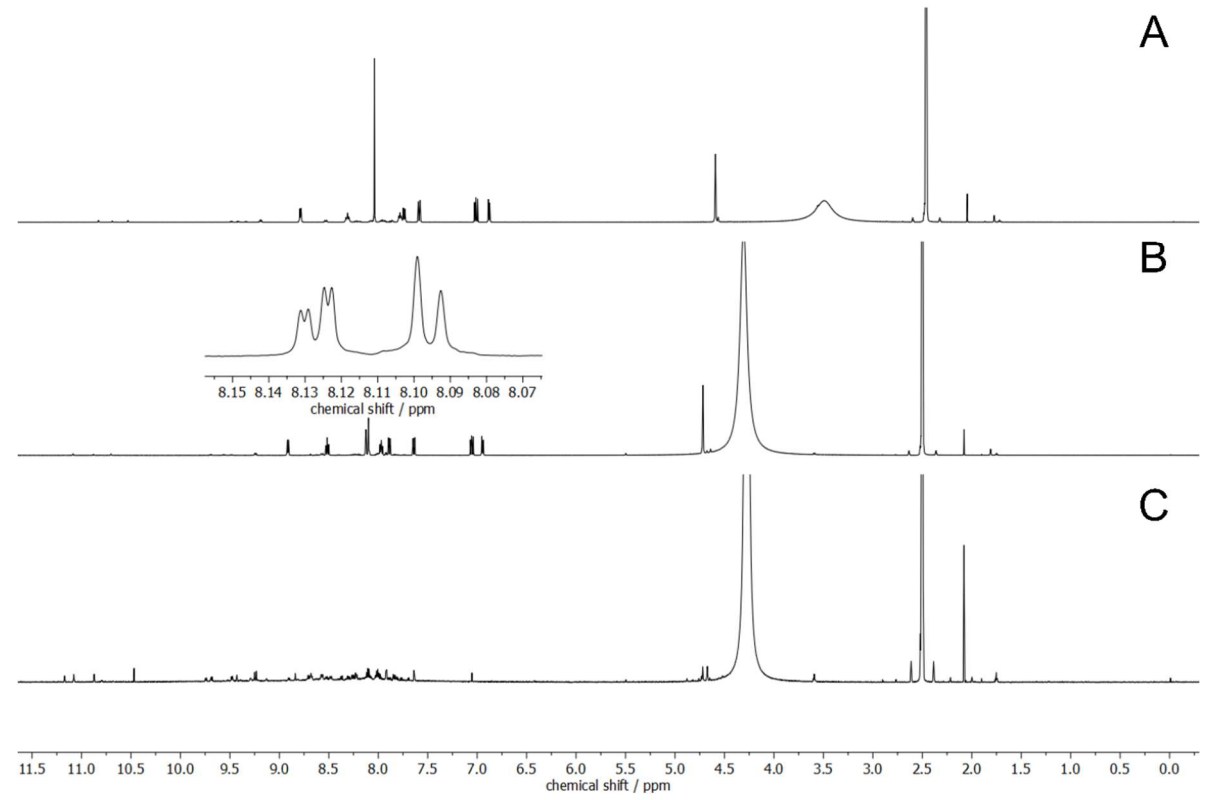

Figure S8. ^{1}H-NMR spectrum (600 MHz, DMSO-d_6, 25 °C) of **3b** after 5 h (A), after addition of 2 equiv. of aq. HBr (48%) (B), and 5 h after addition of aq. HBr (48%) (C).

After addition of hydrobromic acid to the solution of **6** in DMSO-d_6, the proton signal of 1-H and 3-H were resolved into two different signals (Figure S8B) and the spectrum was the same as the one of **6** after chromatographic work up (Figure S42). After addition of an excess of the acid the compound decomposed steadily, and the solution turned black.

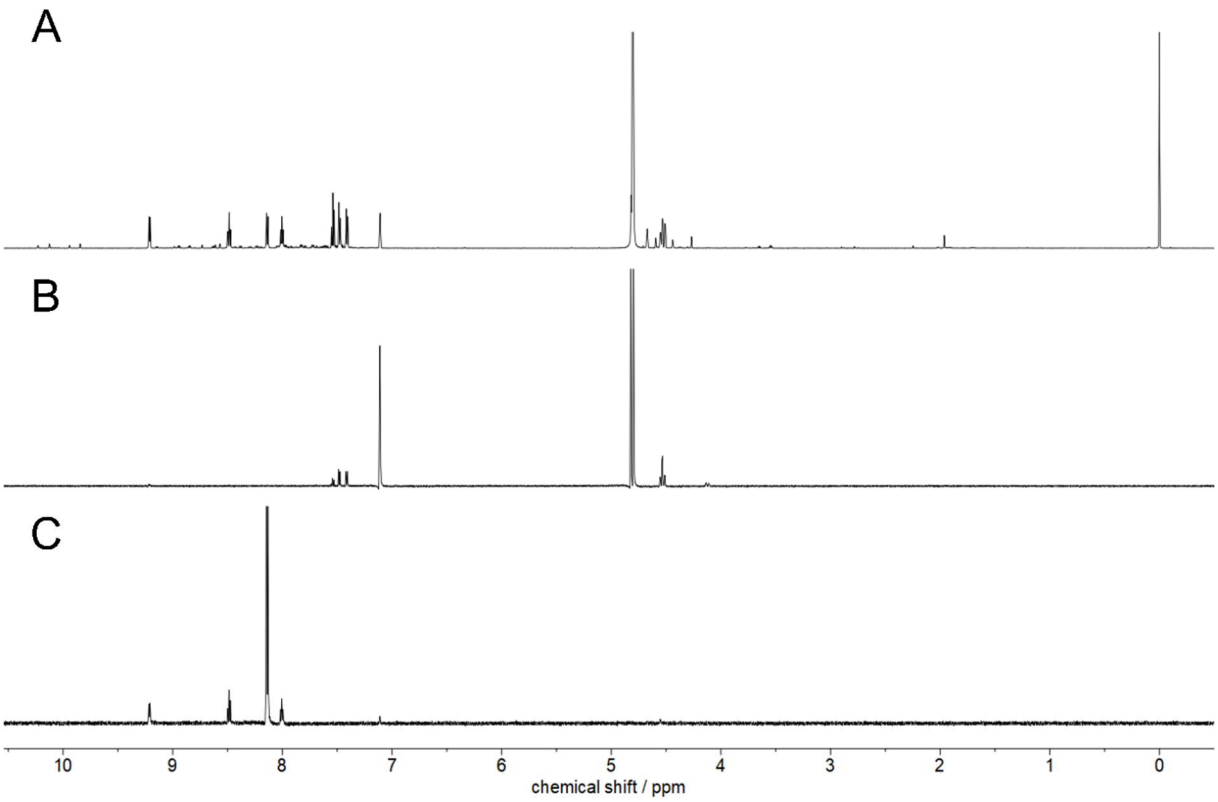

Figure S9. ^{1}H-NMR spectrum (A, 600 MHz, D_2O) and 1D-TOCSY spectrum (B, selective excitation pulse at 4.52 ppm; C, selective excitation pulse at 9.21 ppm) of **3b** directly after sample preparation.

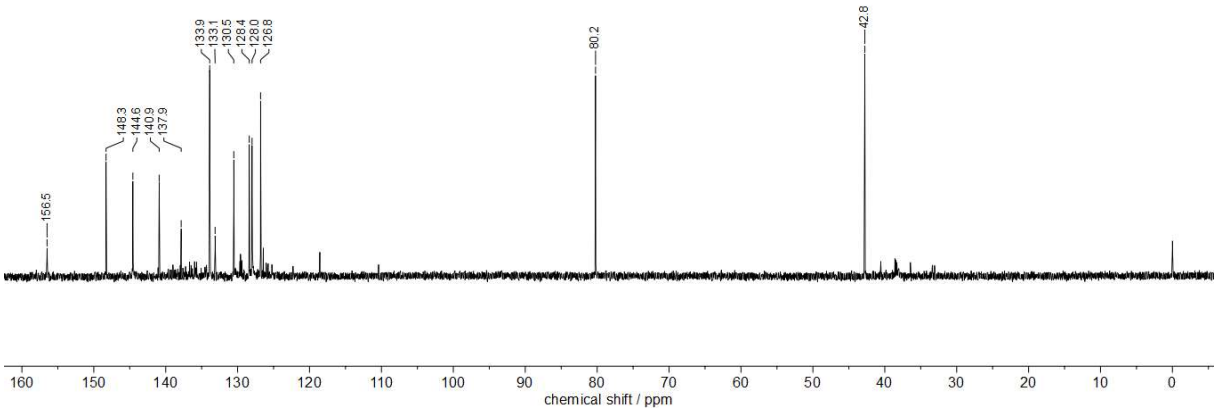

Figure S10. ^{13}C-NMR spectrum (125 MHz, D_2O, 25 °C) of **7** derived from **3b**.

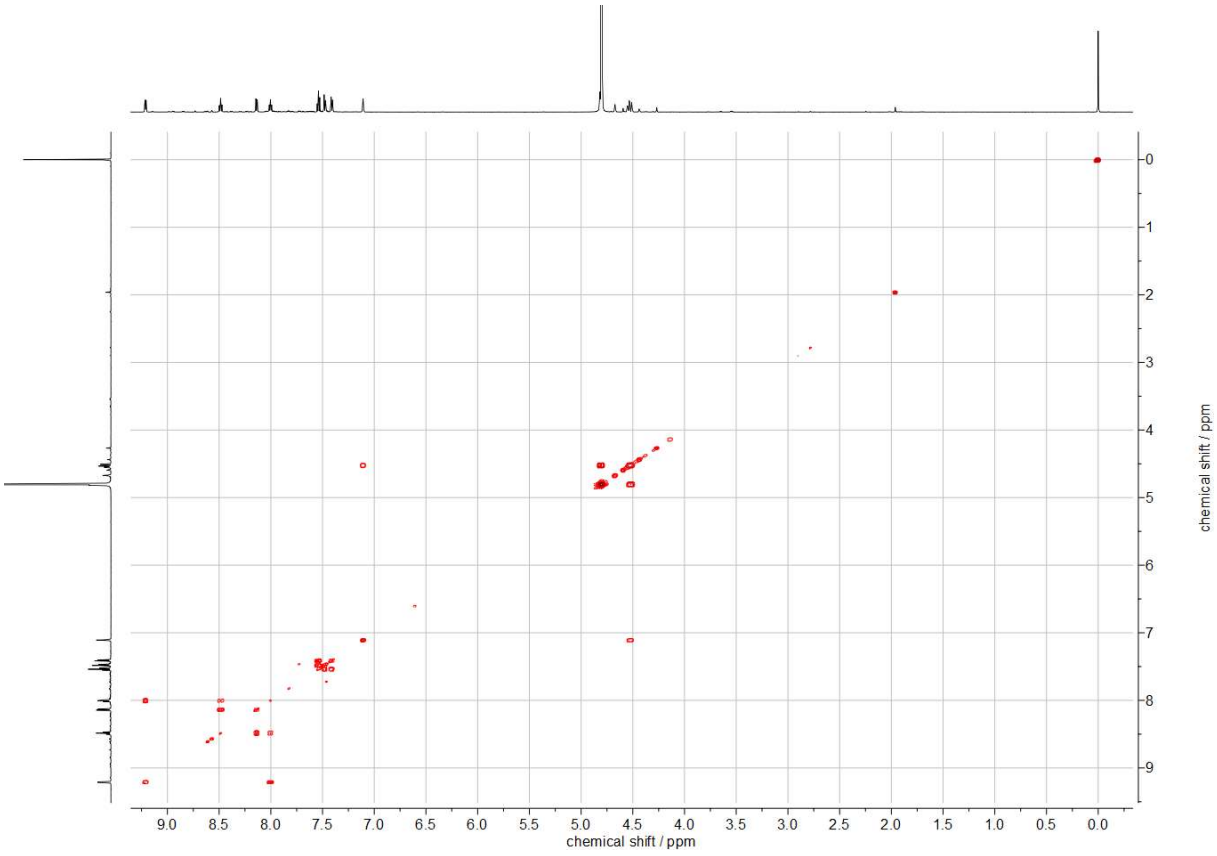

Figure S11. HH-COSY spectrum (500 MHz, D_2O, 25 °C) of **7** derived from **3b**.

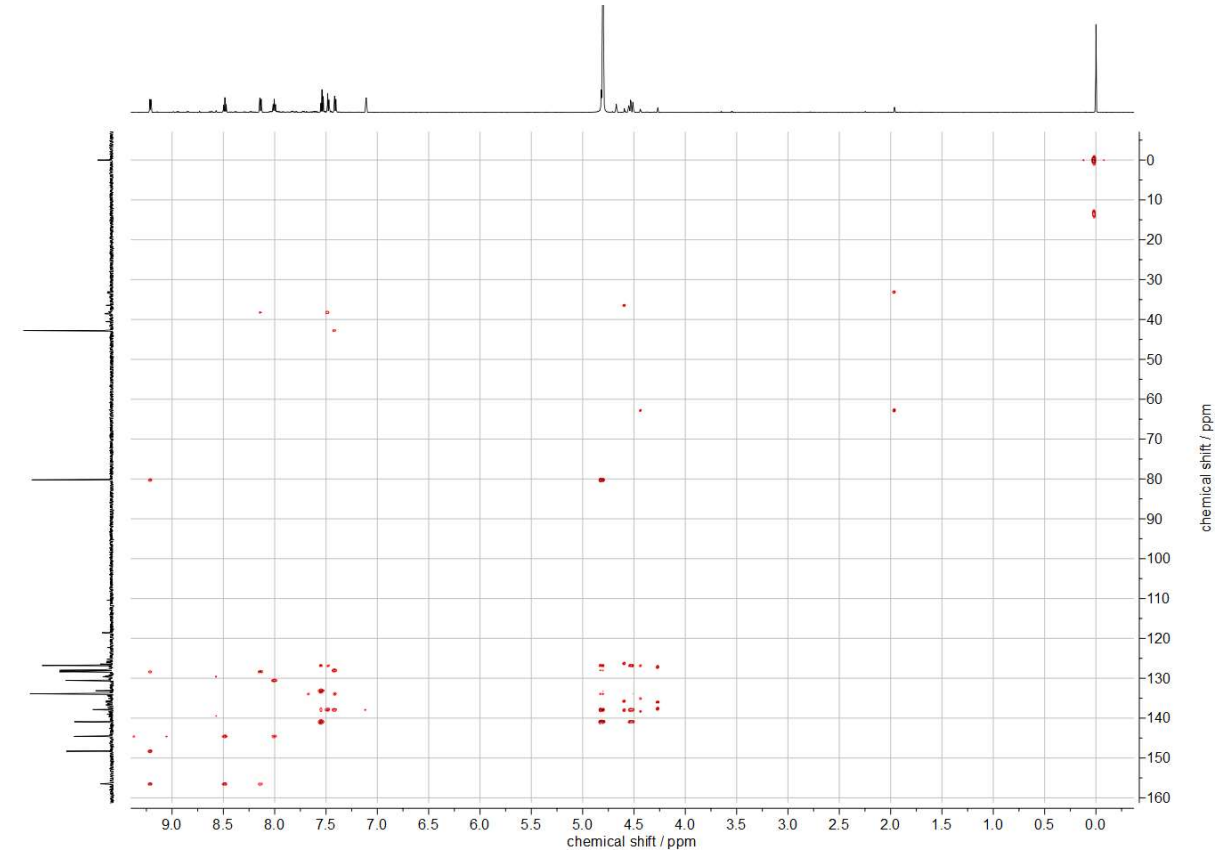

Figure S12. HSQC spectrum (500 MHz, D_2O, 25 °C) of **7** derived from **3b**.

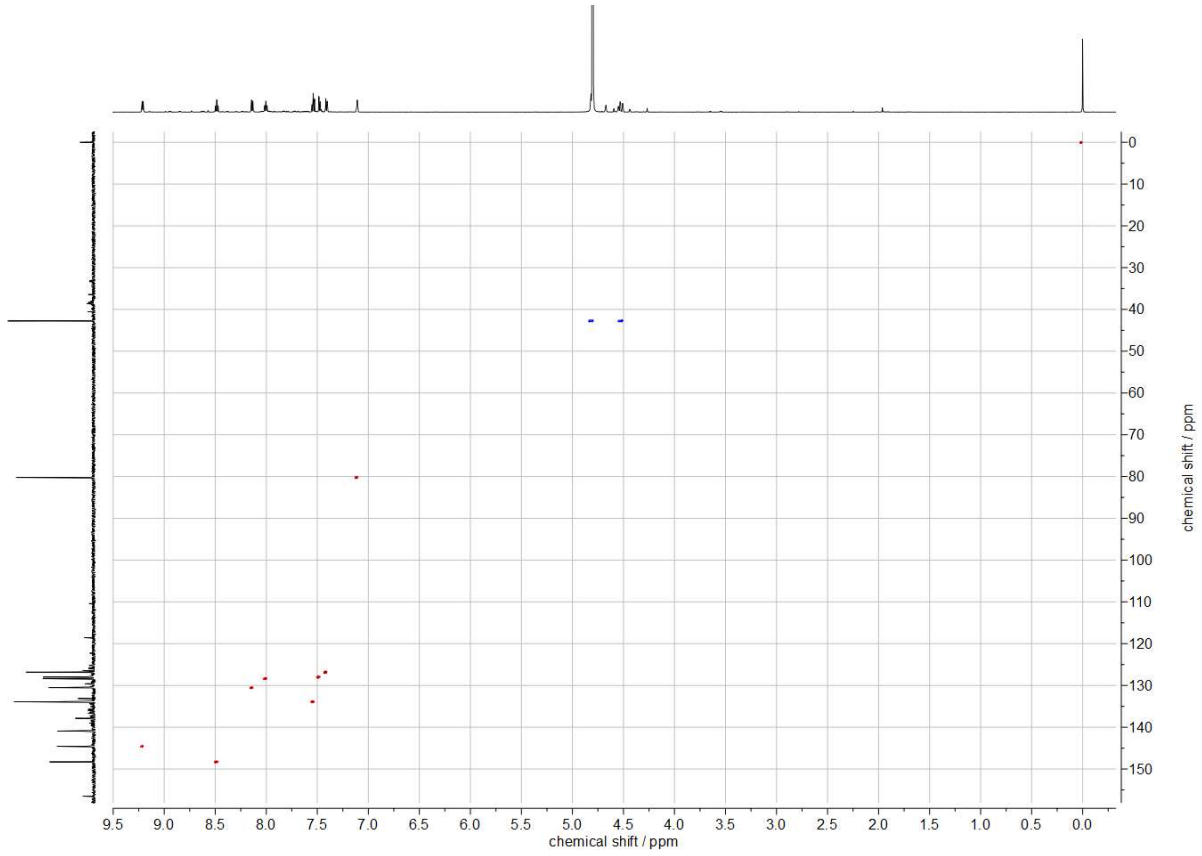

Figure S13. HMBC spectrum (500 MHz, D_2O, 25 °C) of **7** derived from **3b**.

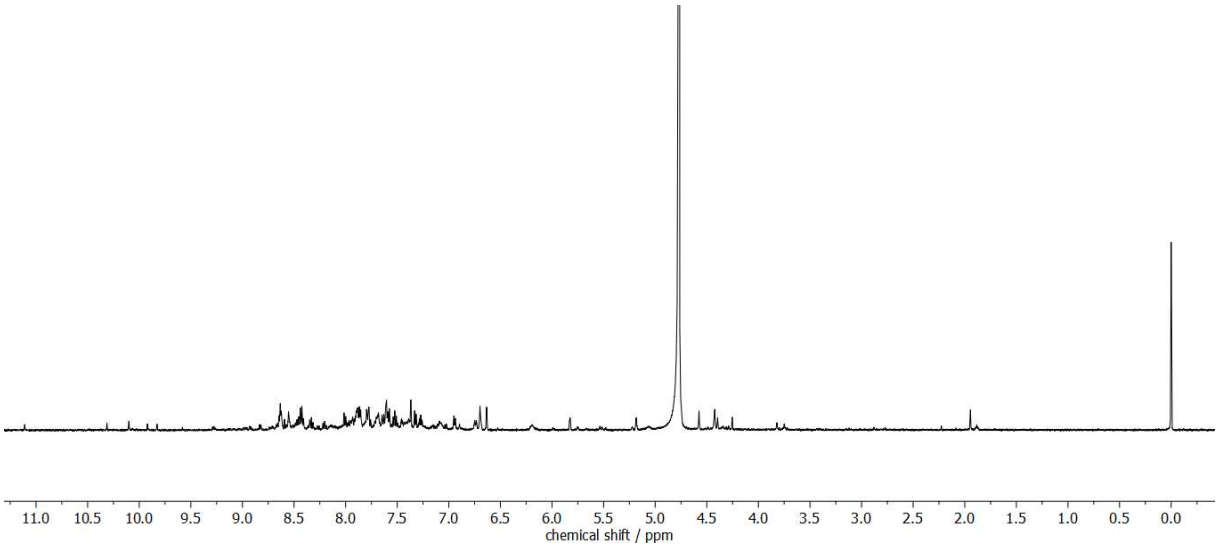

Figure S14. ^{1}H-NMR spectrum (500 MHz, D_2O, 25 °C) of **7** derived from **3b** after 2 d.

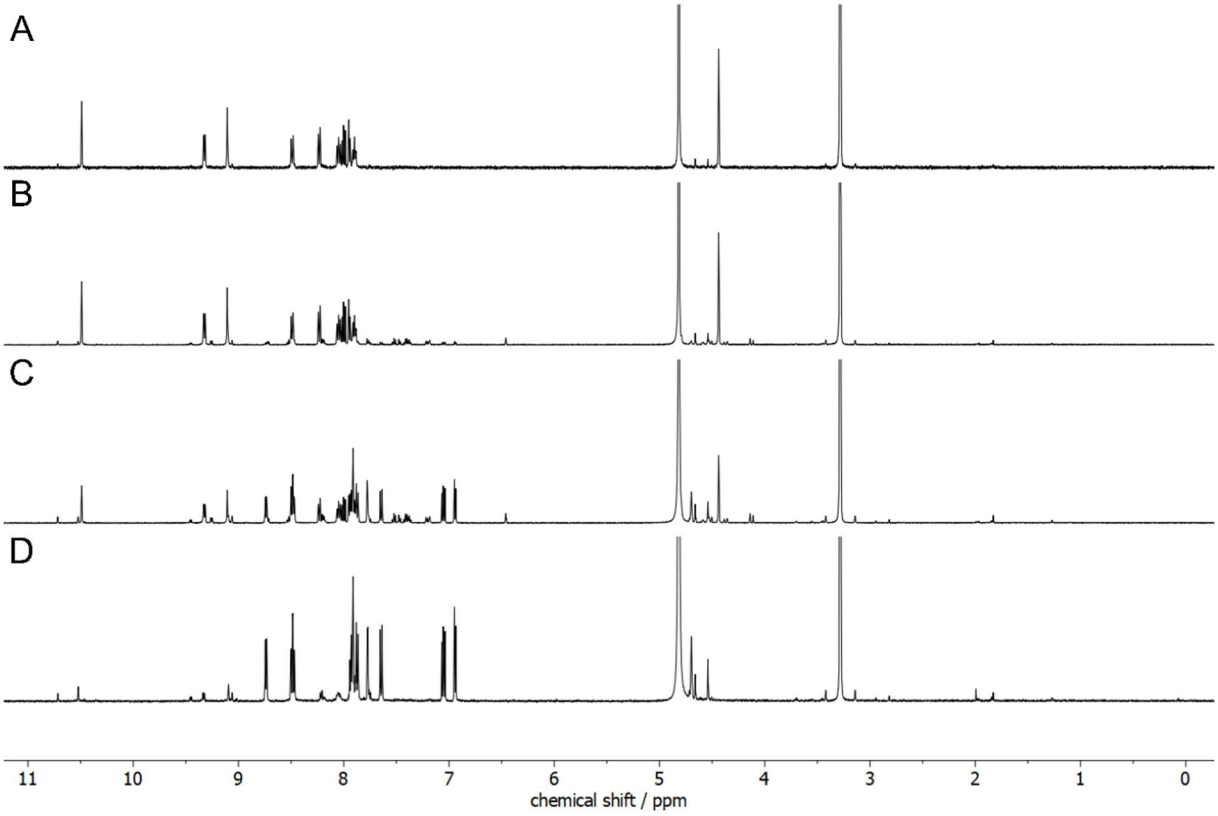

Figure S15. ^{1}H-NMR spectrum (500 MHz, CD_3OD, 25 °C) of **3b** after 3 min (A), 3 h (B), 1 d (C) and 5 d (D).

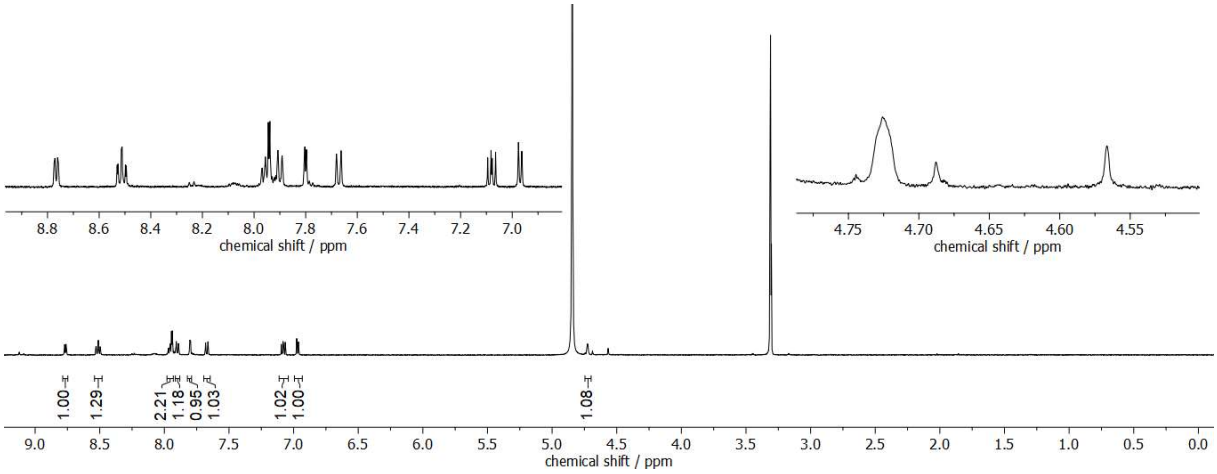

Figure S16. ^{1}H-NMR spectrum (500 MHz, CD_3OD, 25 °C) of **6–D^{+}** derived from **3b**.

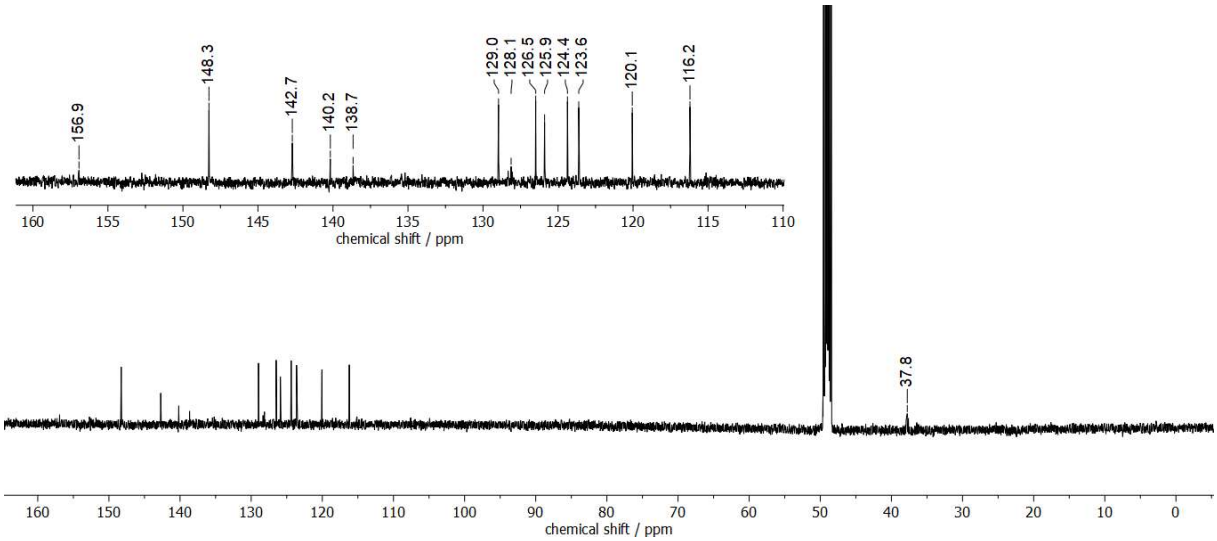

Figure S17. ^{13}C-NMR spectrum (150 MHz, CD_3OD, 25 °C) of **6–D$^+$** derived from **3b**.

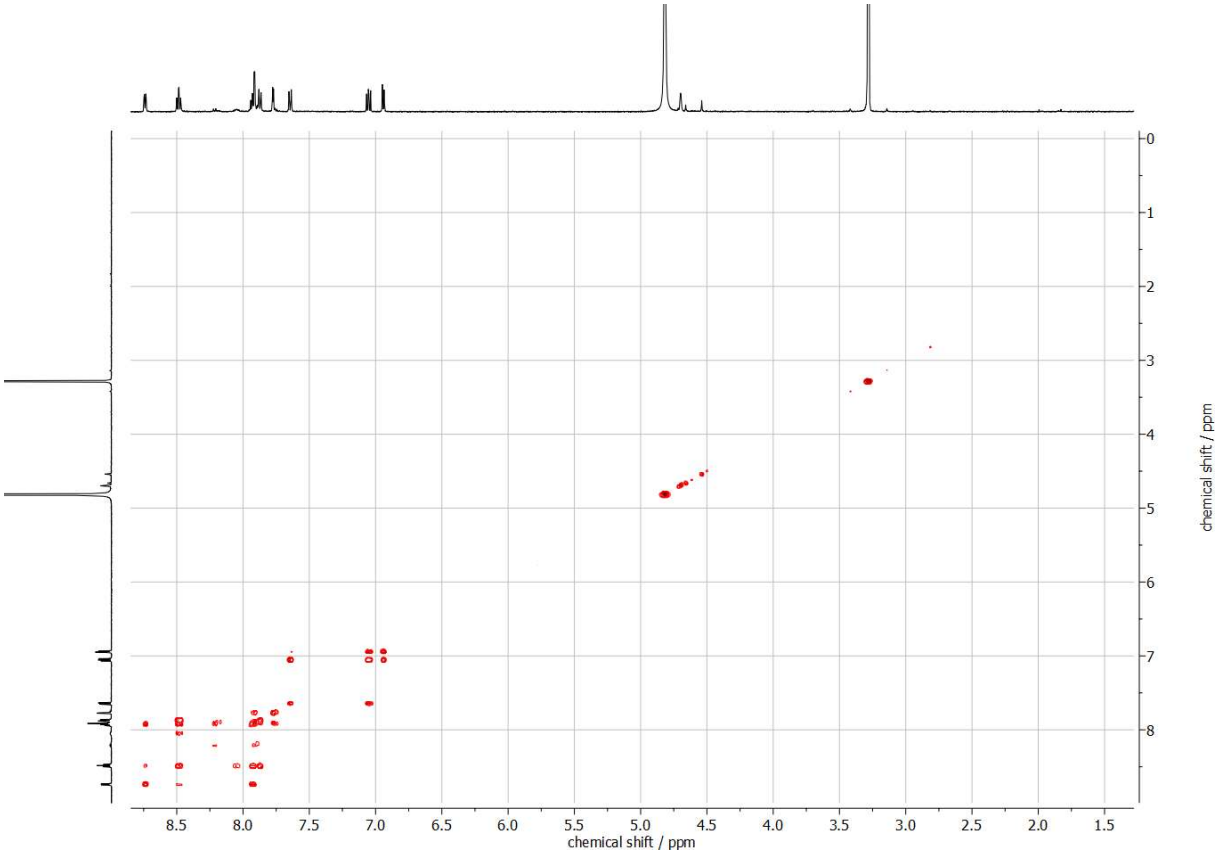

Figure S18. HH-COSY spectrum (500 MHz, CD_3OD, 25 °C) of **6–D$^+$** derived from **3b**.

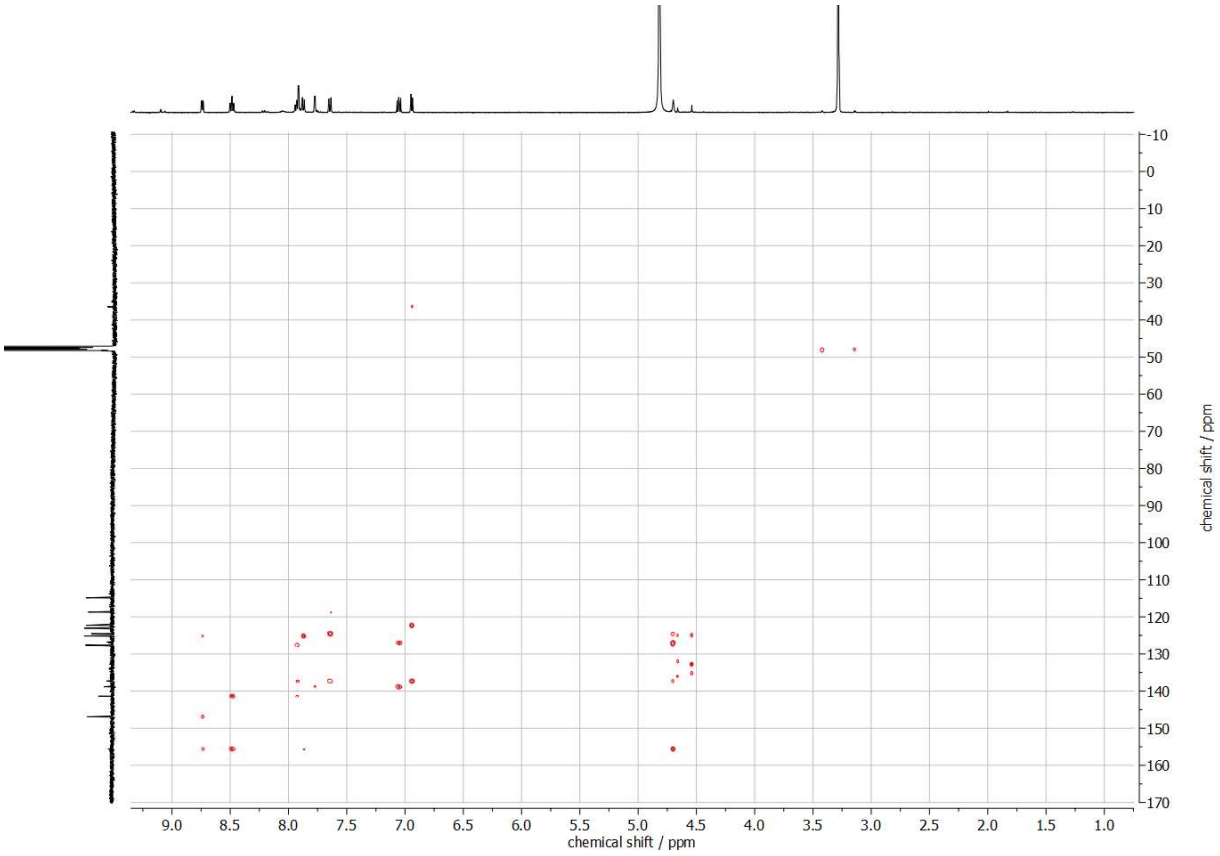

Figure S19. HSQC spectrum (500 MHz, CD_3OD, 25 °C) of **6–D⁺** derived from **3b**.

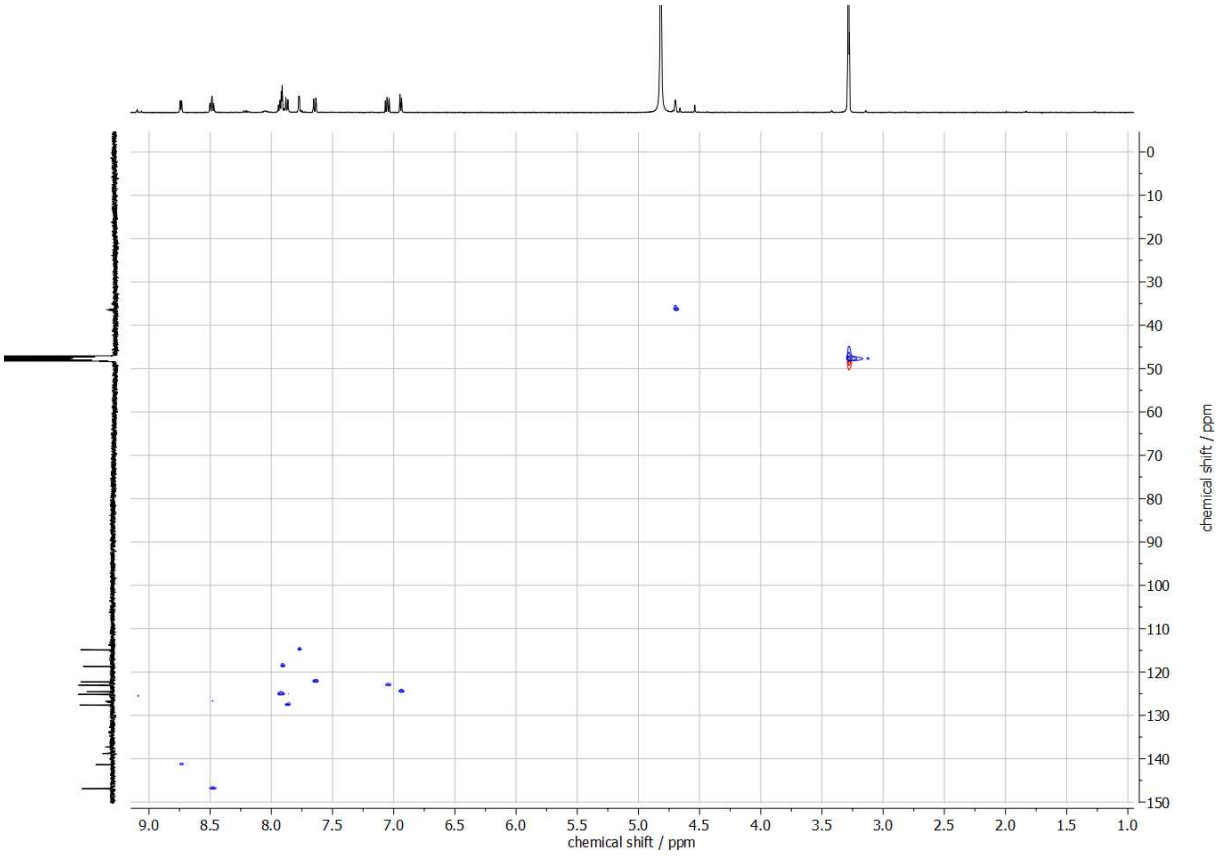

Figure S20. HMBC spectrum (500 MHz, CD_3OD, 25 °C) of **6–D⁺** derived from **3b**.

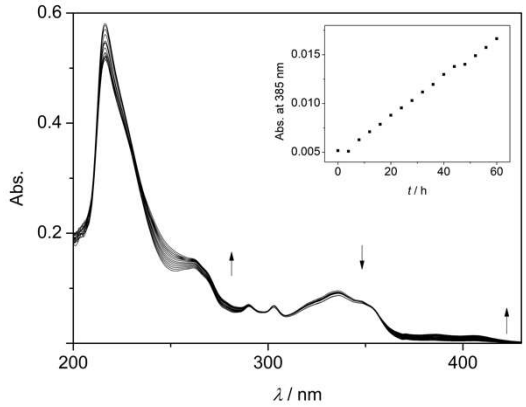

Figure S21. Photometric monitoring of the thermal treatment of **6** (*T* = 37 °C, *c* = 20 µM, acetate buffer, pH = 5.00, *t* = 60 h). Inset: Change of absorbance with time.

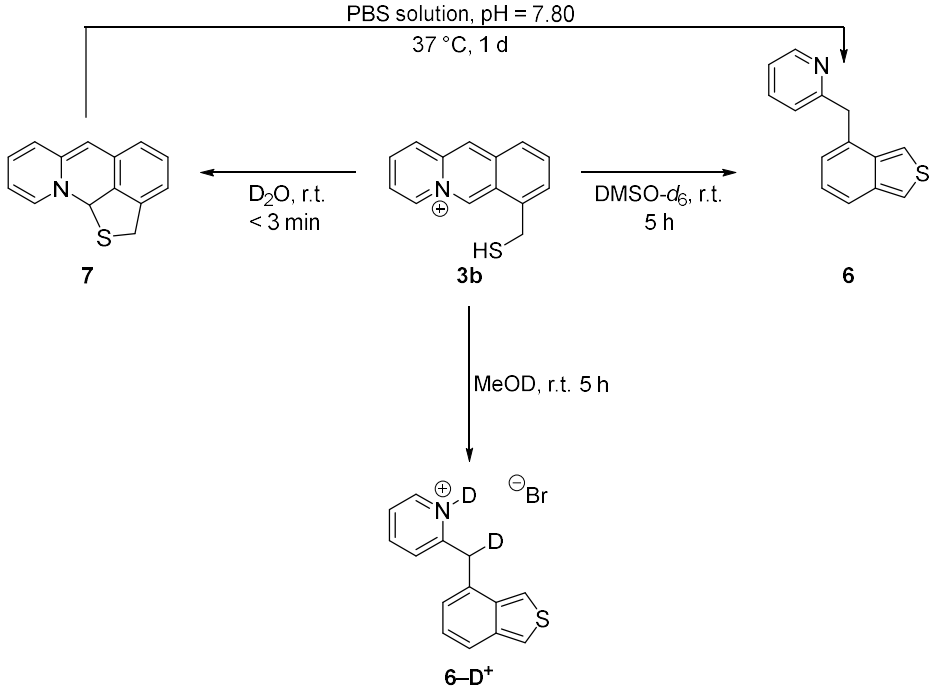

Scheme S1. Reactivity of **3b** in different solvents.

2. Absorption and emission properties

For the measurement of absorption and emission spectra of **2b** and **4b**, aliquots of stock solutions (c = 1 mM, MeOH or MeCN) were evaporated under a stream of nitrogen gas, and the residue was redissolved in the respective solvent. In general, absorption spectra were recorded with a scan rate of 120 nm min^{-1} from 200 to 600 nm and subsequently smoothed with the Origin software (OriginLab, 8.5.1) with the adjacent-averaging function (factor 10). For the detection of emission spectra, the excitation and emission slits were adjusted to 5 nm. The scan rate was 120 nm min^{-1} and the detector voltage was adjusted to 400–800 V. The spectra were smoothed with the implemented moving-average function (factor 5).

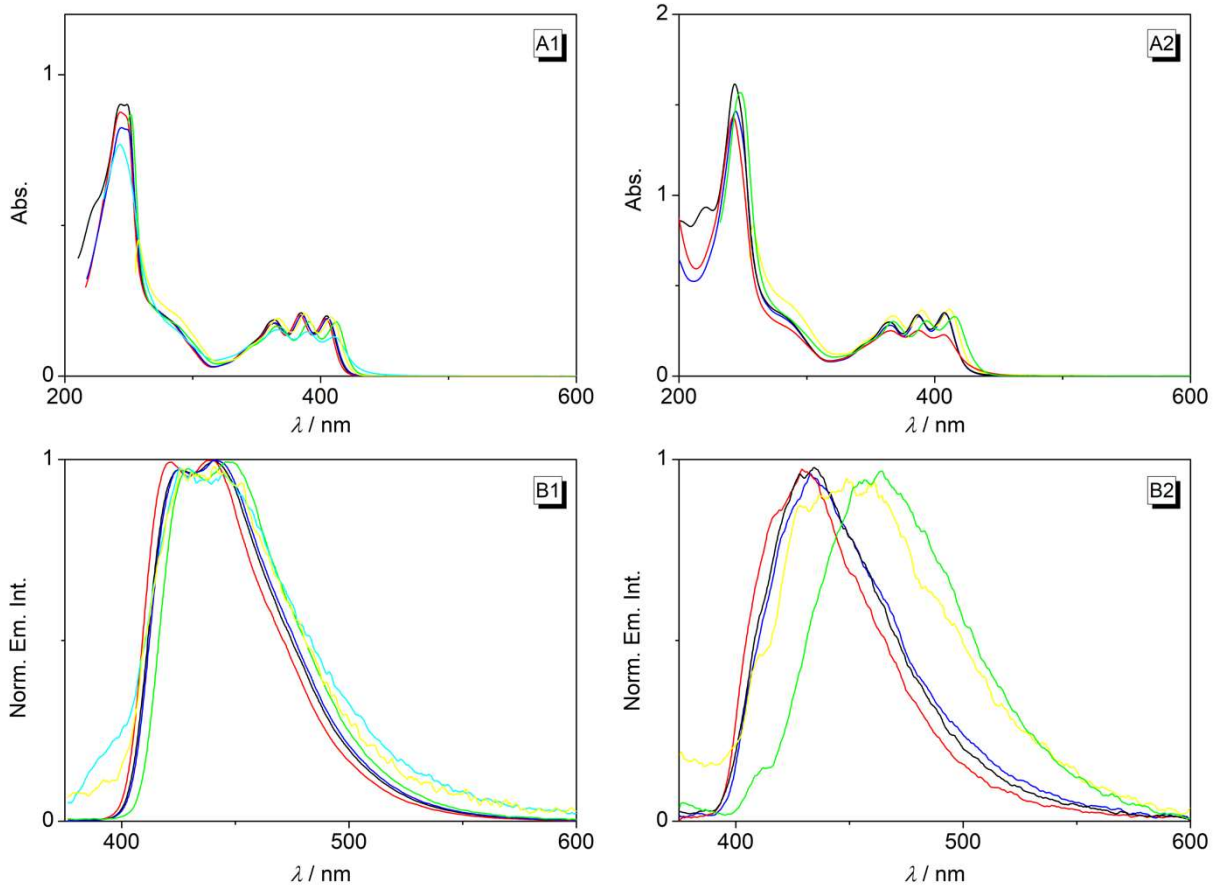

Figure S22. Absorption spectra (c = 20 µM, A) and normalized emission spectra (c = 10 µM, B) of **2b** (1, λ_{ex} = 366 nm) and **4b** (2, λ_{ex} = 365 nm) in CH_2Cl_2 (green), EtOAc (purple), THF (cyan), DMSO (yellow), CH_3CN (black), MeOH (blue), and H_2O (red).

The relative fluorescence quantum yields were determined under identical conditions, i.e., the same cuvettes were used and the measurements were performed at a constant temperature (20 °C) under exclusion of oxygen with the same spectrometer settings (detection wavelength, excitation wavelength, detector voltage, slit bandwidths, collection rate). Anthracene (Φ_{Fl} =

0.28 in cyclohexane, λ_{ex} = 340 nm[1]) was used as standard. The emission spectra were collected from solutions with Abs. = 0.10 at the excitation wavelength. After integration of the fluorescence band, the relative fluorescence quantum yields were calculated according to eq. 1.

$$\phi_{Fl} = \frac{J_x\,(1 - T_s)\,n_x^2}{J_s\,(1 - T_x)\,n_s^2} \cdot \phi_{Fl,s} \qquad \text{(eq. 1)}$$

The subscripts "x" and "s" refer to the substance under investigation and the reference compound, respectively; $J = \int I_{Fl}(\lambda)\,d\lambda$ is the integral of the emission band; T is the optical transmittance of the sample solution at the excitation wavelength λ_{ex}; n is the refractive index of the sample or standard solution.

Table S1. Absorption and emission properties of compound **2b**.

Solvent	Absorption		Fluorescence	
	λ_{abs} / nm[a]	lg ε[b]	λ_{Fl} / nm[c]	Φ_{Fl}[d]
DCM	412	3.95	446	0.05
THF	411	3.81	426	<0.01
DMSO	408	3.99	440	0.01
CH_3CN	405	4.00	440	0.24
MeOH	406	3.98	440	0.24
H_2O	404	3.98	440	0.25

[a] Long-wavelength absorption maximum. [b] Molar extinction coefficient in $cm^{-1}\,M^{-1}$. [c] Fluorescence maximum, λ_{ex} = 366 nm. [d] Relative to anthracene Φ_{Fl} = 0.28 (EtOH, λ_{ex} = 340 nm, Ref. 1).

Table S2. Absorption and emission properties of compound **4b**.

Solvent	Absorption		Fluorescence	
	λ_{abs} / nm[a]	lg ε[b]	λ_{Fl} / nm[c]	Φ_{Fl}[d]
DCM	416	4.22	464	<0.01
DMSO	411	4.27	448	<0.01
CH_3CN	408	4.24	435	<0.01
MeOH	409	4.23	433	<0.01
H_2O	408	4.06	429	<0.01

[a] Long-wavelength absorption maximum. [b] Molar extinction coefficient in $cm^{-1}\,M^{-1}$. [c] Fluorescence maximum λ_{ex} = 366 nm. [d] Relative to anthracene Φ_{Fl} = 0.28 (EtOH, λ_{ex} = 340 nm, Ref. 1).

3. Photoreactions of 4b

3.1 Photometric monitoring of the photoreaction of 4b and thermal stability of the photoproduct

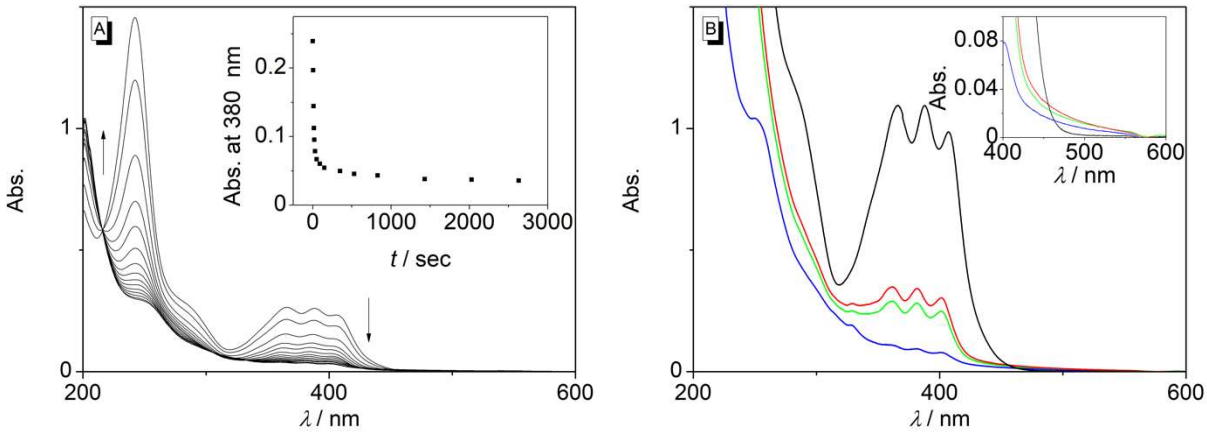

Figure S23. A: Photometric monitoring of the photoreaction of **4b** in H_2O (c = 20 µM) with λ_{ex} = 365 nm. B: Photometric monitoring of the photoreaction of **4b** in H_2O (c = 80 µM) with λ_{ex} = 365 nm at t = 0 s (black) and t = 90 min (blue) and further irradiation with λ_{ex} = 310 nm at t = 5 min (green) and t = 15 min (blue). Inset A: Change of absorbance at the long wavelength absorption maximum during irradiation. Inset B: Magnification of the absorbance at 400–600 nm.

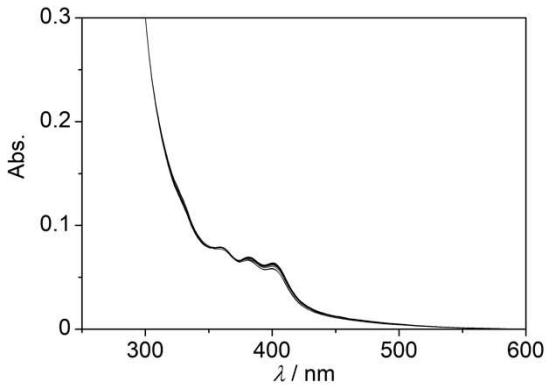

Figure S24. Photometric monitoring of **4b^{shh}** and **c4b^{ahh}** (c = 40 µM, derived from irradiation of **4b** with λ_{ex} = 365 nm, t = 30 min) in PBS solution (pH = 7.0) in the presence of DNA (c = 160 µM) at 37 °C for 16 h.

3.2 NMR-spectroscopic analysis of the photoreaction

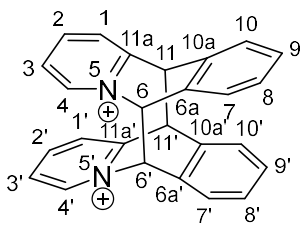

Figure S25. General numbering of the photodimer of benzo[*b*]quinolizinium (**1**).

A solution of **4b** (1.6 mg, 2.6 µmol) in D_2O (500 µL) was irradiated in a NMR tube (λ_{exc} = 365 nm) for 13 min.

4b^{ahh}:

^{1}H-NMR (600 MHz, D_2O, 40 °C): δ = 4.11, 4.36 [AB system, ^2J = 15 Hz, 4H, 2 × C7-CH_2], 5.78 (s, 2H, 2 × 11-H), 7.17 (dd, ^3J = 7 Hz, ^4J = 2 Hz, 2H, 2 × 10-H), 7.20–7.26 (m, 4H, 2 × 8-, 2 × 9-H), 7.40 (s, 2H, 2 × 6-H), 7.87–7.93 (m, 2H, 2 × 3-H), 8.17 (d, ^3J = 8 Hz, 2H, 2 × 1-H), 8.50 (ddd, ^3J = 9 Hz, ^3J = 8 Hz, ^4J = 1 Hz, 2H, 2 × 2-H), 9.07 (d, ^3J = 6 Hz, 2H, 2 × 4-H). – ^{13}C NMR (150 MHz, D_2O, 40 °C): δ = 36.0 (2 × C7-CH_2), 52.6 (2 × C11), 72.1 (2 × C6), 130.2 (2 × C3), 130.4 (2 × C9, 2 × C10), 131.7 (2 × C1), 132.9 (2 × C8), 133.8 (2 × C6a), 135.1 (2 × C10a), 139.7 (2 × C7), 148.7 (2 × C4), 151.6 (2 × C2), 157.7 (2 × C11a).

4b^{shh}:

^{1}H-NMR (600 MHz, D_2O, 40 °C): δ = 4.00, 4.17 [AB system, ^2J = 15 Hz, 4H, 2 × C7-CH_2], 5.85 (s, 2H, 2 × 11-H), 7.12 (d, ^3J = 8 Hz, 2H, 2 × 8-H), 7.20–7.26 (m, 2H, 2 × 9-H), 7.35 (d, ^3J = 8 Hz, 2H, 2 × 10-H), 7.50 (s, 2H, 2 × 6-H), 7.87–7.93 (m, 2H, 2 × 3-H), 8.14 (d, ^3J = 8 Hz, 2H, 2 × 1-H), 8.48 (td, ^3J = 8 Hz, ^4J = 1 Hz, 2H, 2 × 2-H), 9.21 (d, ^3J = 6 Hz, 2H, 2 × 4-H). – ^{13}C NMR (150 MHz, D_2O, 40 °C): δ = 36.0 (2 × C7-CH_2), 52.8 (2 × C11), 73.3 (not visible in ^{13}C-NMR spectrum, but visible in HMBC, 2 × C6),130.1 (2 × C3),131.4 (not visible in ^{13}C-NMR spectrum, but visible in HSQC experiment, 2 × C10),131.6 (2 × C1),134.0 (2 × C9),134.4 (not visible in ^{13}C-NMR spectrum, but visible in HMBC experiment, 2 × C8),137.5 (2 × C10a),148.8 (2 × C4),151.4 (2 × C2),157.6 (2 × C11a). Comment: No ^{13}C-NMR signal could be assigned to C7' and C6a'. – HRMS (ESI$^+$): Calcd for: $[C_{28}H_{22}N_2S_2]^{2+}$ *m/z* = 225.0607, found: 225.0608 [M].

4. Thioester cleavage of 2b by esterase

A solution of **2b** (*c* = 20 µM) in PBS solution (pH = 7.80) was treated with esterase from porcine liver (400 µg, 7.6 units) for 22 h at 37 °C, and the reaction was followed photometrically by measuring an absorption spectrum every 20 min (*cf*. main manuscript, Figure S24).

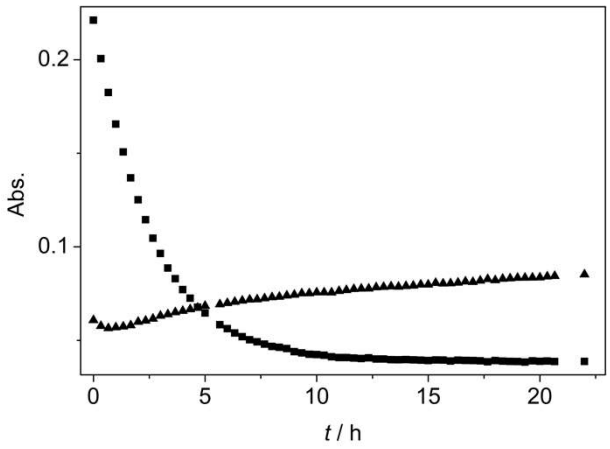

Figure S26. A2: Photometric monitoring of the reaction of **2b** (*c* = 20 µM) with esterase (400 µg, 7.6 Units) for 22 h at 37 °C in PBS solution (pH = 7.80) presented as plot of absorption at 403 nm (squares) and 323 nm (triangles) versus *t*.

5. DNA-binding studies

5.1 Photometric and fluorimetric titrations

To solutions of **2b** (λ_{ex} = 412 nm), **4b** (λ_{ex} = 365 nm), **6** (λ_{ex} = 335 nm), and **c4b^{shh}** (λ_{ex} = 360 nm) (*c* = 20 µM) in BPE buffer (pH = 7.00) were added aliquots of a ct DNA stock solution, and the respective absorption and emission spectra (Figure S25) were recorded after an equilibration time of 3 min. The titration was stopped when at least four equivalents of DNA were added, or no more significant changes were observed during photometric titrations upon addition of DNA.

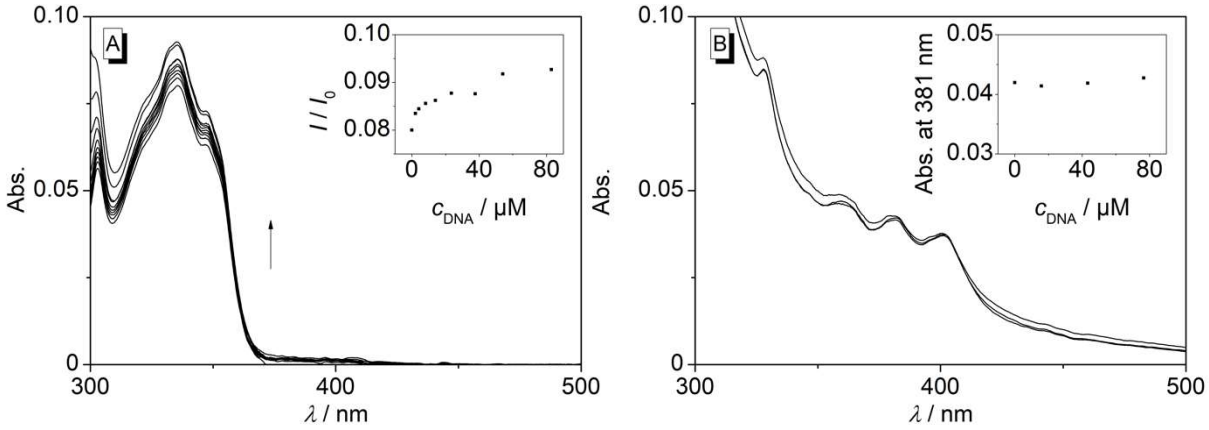

Figure S27. Photometric titrations of **6** (A) and **c4b^{shh}** and **c4b^{ahh}** (B) (*c* = 20 µM) with ct DNA in bisphosphate EDTA (BPE) buffer (pH = 7.00); The arrows indicate the change of the absorption bands during titration. Insets: Plots of the changes of absorption or fluorescence upon addition of DNA.

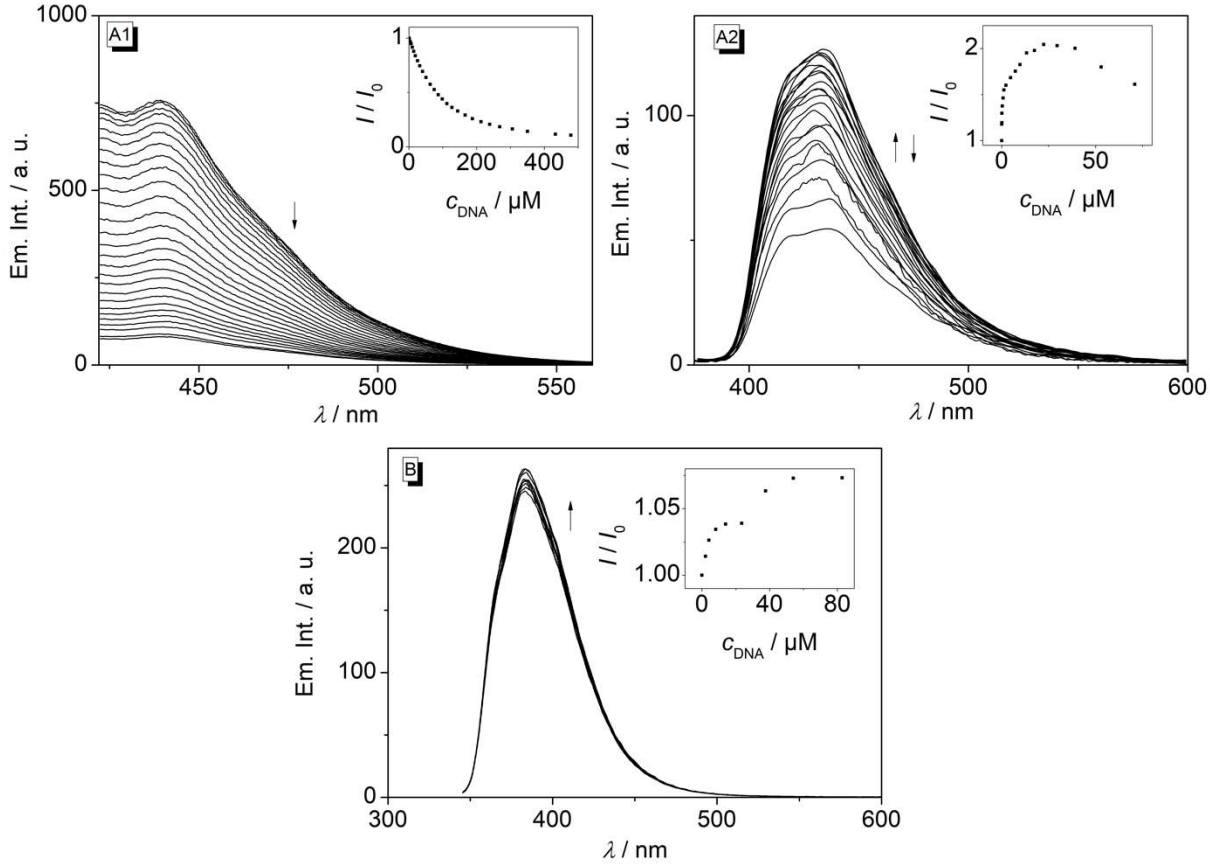

Figure S28. Fluorimetric titrations of **2b** (A1, λ_{ex} = 412 nm), **4b** (A2, λ_{ex} = 365 nm), **6** (1, λ_{ex} = 335 nm), with ct DNA in BPE buffer (c_{ligand} = 20 µM, pH = 7.00). The arrows indicate the change of the fluorescence from the first to the last titration step. Insets: Plot of the change of fluorescence intensity versus c_{DNA}.

5.2 Fluorescent indicator displacement (FID) assay

For compound **4b** a fluorescent indicator displacement (FID) experiment with thiazol orange (**TO**) was performed according to known procedure.[Fehler! Textmarke nicht definiert.] To a solution of **TO** (0.5 µM) and ct DNA (0.25 µM) in BPE buffer (pH = 7.00) were added aliquots of a stock solution of **4b** (c = 50 µM), in BPE buffer, and the fluorescence (λ_{ex} = 475 nm) was recorded after an equilibration time of 3 min. The percentage displacement (PD) of **TO** and the PD50 value (PD = 50%) were calculated according to equation 2.

$$PD = 100 - \left(\frac{FA}{FA_0} \times 100\right) \qquad \text{(eq. 2)}$$

The variable FA refers to the fluorescence area (500–750 nm) at the respective titration step and FA_0 refers to the fluorescence area before the addition of the ligand.

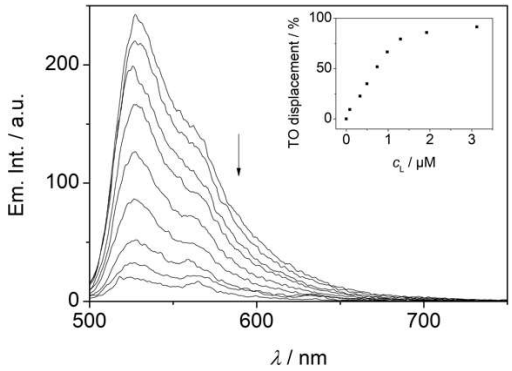

Figure S29. Changes of the fluorescence spectra (λ_{ex} = 475 nm) of **TO** (0.5 μM) bound to DNA (0.25 μM) upon addition of **4b** in BPE buffer (pH = 7.00). The arrow indicates the change of the fluorescence from the first to the last titration step. Inset: **TO** displacement versus concentration of the added ligand.

5.3 CD- and LD-spectroscopic analysis

Solutions of ct DNA (*c* = 50 μM) with different concentrations of **2b**, **4b**, **6,** or **c4b^{shh}** and **c4b^{ahh}** in BPE buffer (pH = 7.0) were prepared and analyzed by CD (Figure S27) and LD spectroscopy (Figure S28). The solutions of the photoproduct of **2b** were prepared by irradiation of solutions of **2b** (λ_{ex} = 365 nm, *t* = 3 min) prior to the addition of DNA.

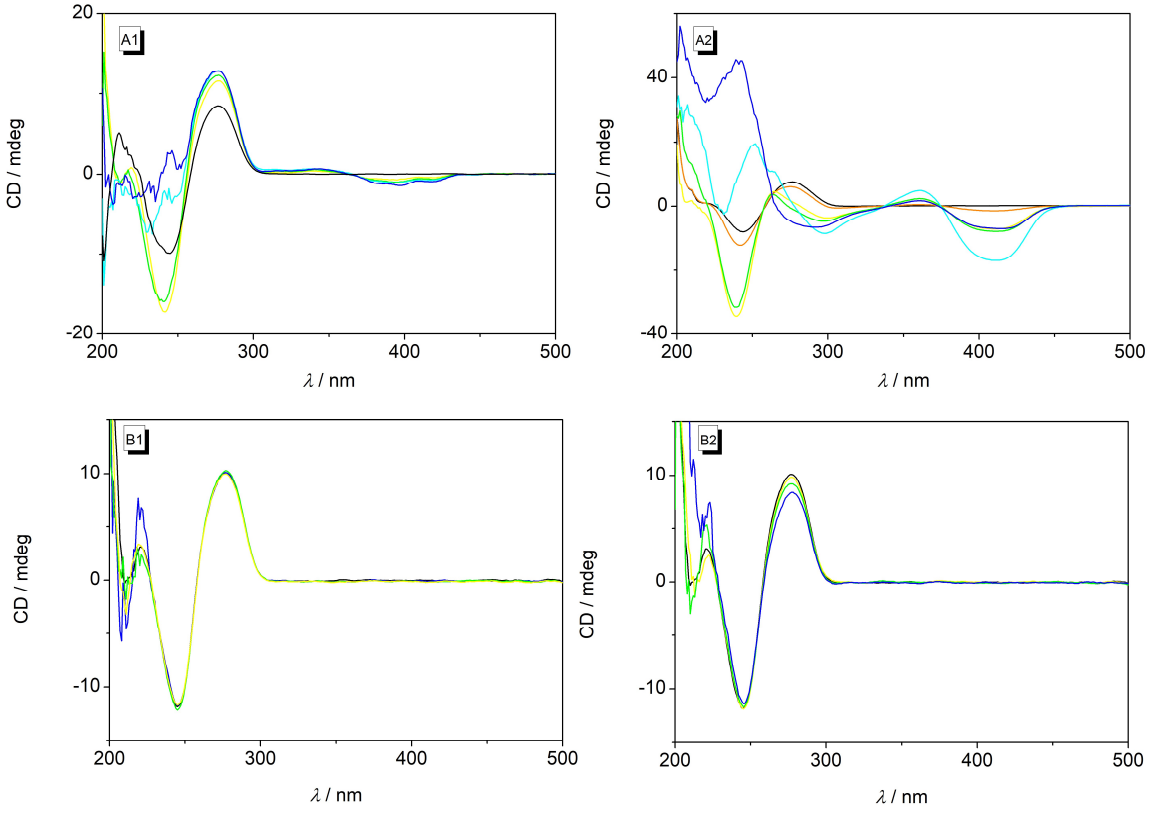

Figure S30. CD spectra of **2b** (A1), **4b** (A2), **6** (B1), and **c4b^{shh}** and **c4b^{ahh}** (B2) in BPE buffer (pH = 7.00) with ct DNA (*c* = 50 μM) at different ligand-DNA ratios [LDR = 0 (black), 0.1 (orange), 0.5 (yellow),1.0 (green), 1.5 (cyan), 2.0 (blue)].

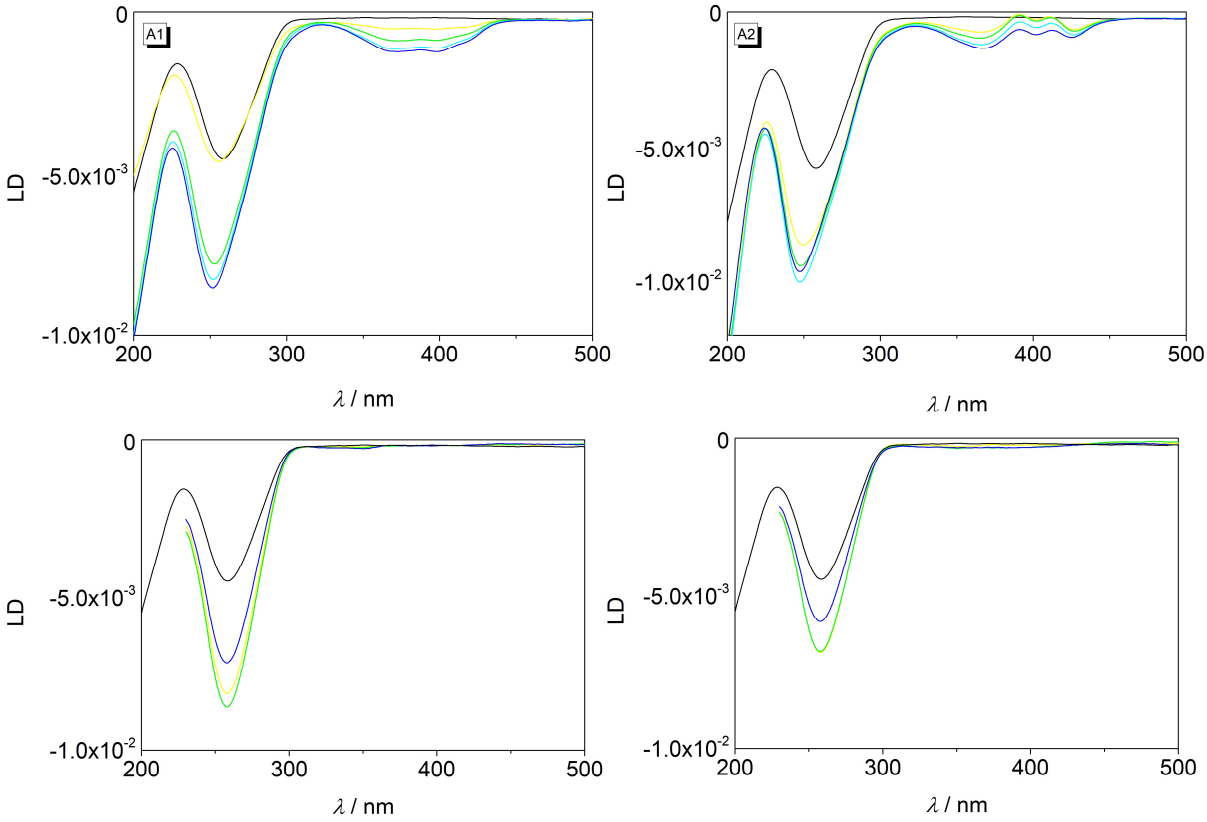

Figure S31. LD spectra of **2b** (A1), **4b** (A2), **6** (B1), and **c4b^{shh}** and **c4b^{ahh}** (B2) in BPE buffer (pH = 7.00) with ct DNA (*c* = 50 μM) at different ligand-DNA ratios [LDR = 0 (black), 0.1 (orange), 0.5 (yellow), 1.0 (green),1.5 (cyan), 2.0 (blue)].

5.4 Determination of binding constants

The binding constants were determined by fitting of the respective saturation fraction (SF, eq. 3) calculated from the photometric titrations according to literature protocol (eq. 4).[2]

$$SF = \frac{Abs_n - Abs_0}{Abs_s - Abs_0} \qquad \text{(eq. 3)}$$

The variable Abs_n is the absorption at the titration step n, Abs_0 is the absorption with n = 0 and Abs_s is the absorption when all ligands are bound to the DNA (assessed by analysis of photometric data, often last titration step).

$$y = \frac{1}{2} R\,(A + B + x - \sqrt{(((A + B + x)^2) - (4Bx))}) \qquad \text{(eq. 4)}$$

The variable R refers to an instrumental response sensitivity dependent variable, A is the reciprocal binding constant K_b, B is a dependent variable and is equal to the concentration of the ligand or the DNA (equal to ligand concentration if DNA is added to the ligand and vice versa).

Table S3. Parameters of the fit of experimental titration data to the theoretical Model (eq. 4, Figure S31).

Ligand	A[d]	B[e]	R[f]
4b[a]	1.63×10^{-6}	5.00×10^{-5}	2.03×10^{4}
2b[b]	4.95×10^{-5}	6.00×10^{-5}	1.88×10^{4}
2b[c]	5.07×10^{-5}	6.00×10^{-5}	1.87×10^{4}

[a] Derived from polarimetric DNA titration (CD spectroscopy). [b] Derived from photometric titration. [c] [d] Dependent variable A = K_b^{-1}. [e] Independent variable, fixed according to concentration of the ligand/DNA and theoretically available binding sites. [f] Dependent instrumental response sensitivity variable.

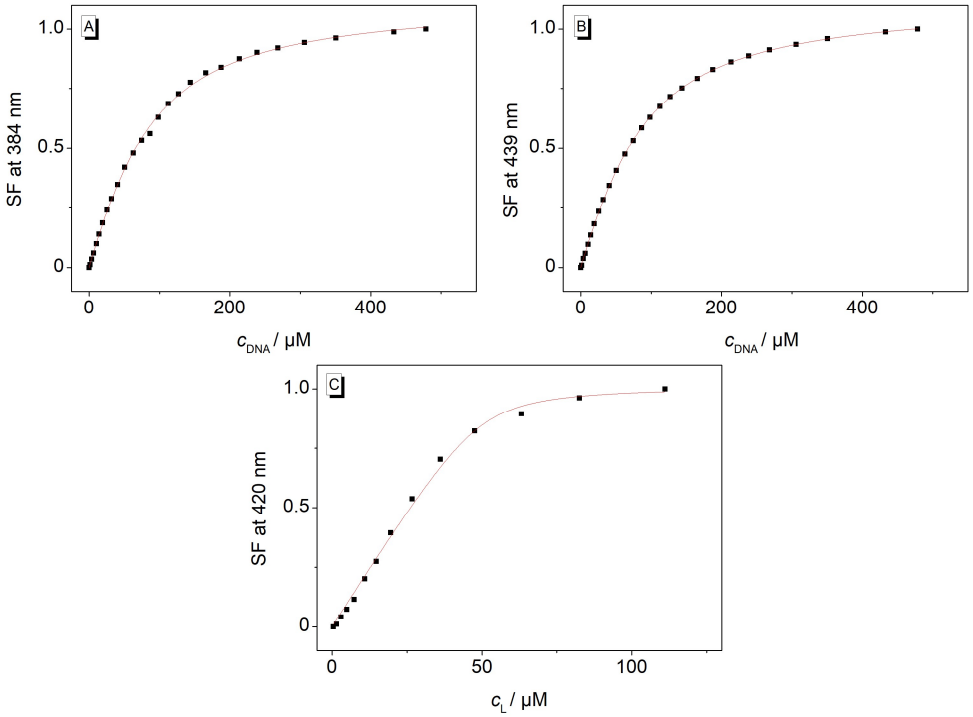

Figure S32. Plot of saturation fraction versus DNA concentration c_{DNA} (A, B) or versus ligand concentration c_L (C) and the resulting binding isotherms of **2b** (A, photometric, B, fluorimetric) and **4b** (C, polarimetric) from corresponding Levenberg–Marquardt least-square fitting curves Ref. 2 of the respective spectroscopic titration approach.

6. NMR spectra of 2b, 3b, 4b and 6

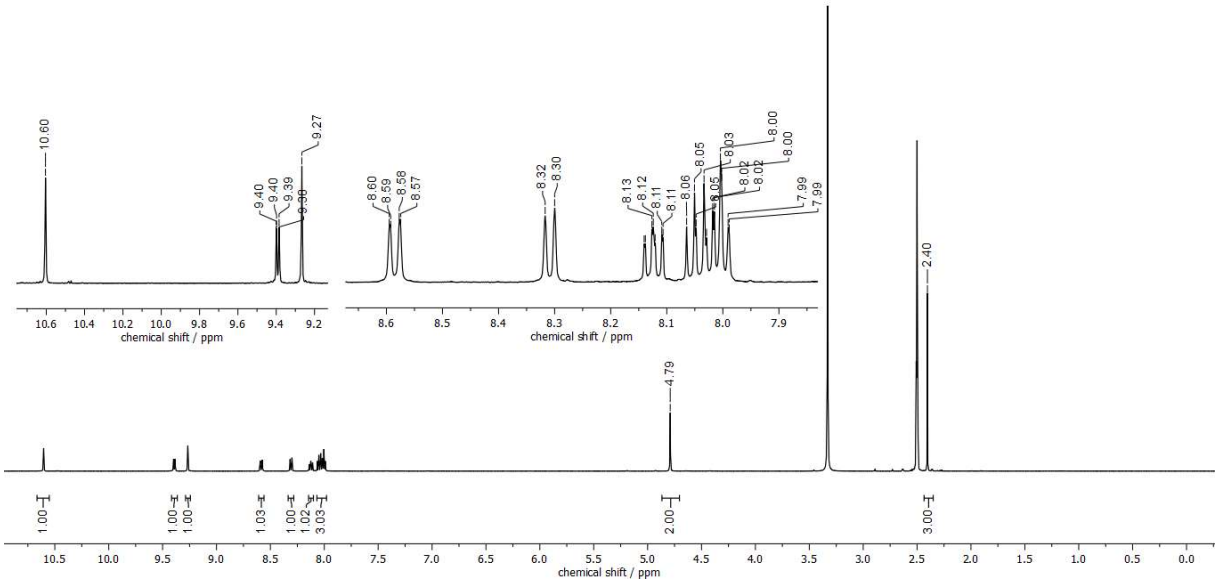

Figure S33. ^{1}H-NMR spectrum (500 MHz, DMSO-d_6, 25 °C) of **2b**.

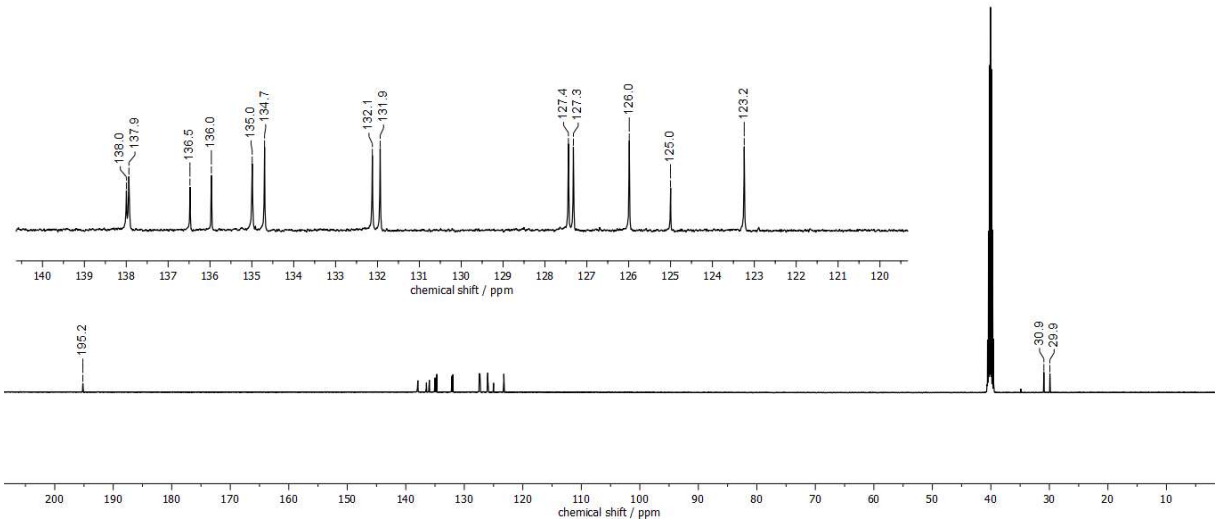

Figure S34. ^{13}C-NMR spectrum (500 MHz, DMSO-d_6, 25 °C) of **2b**.

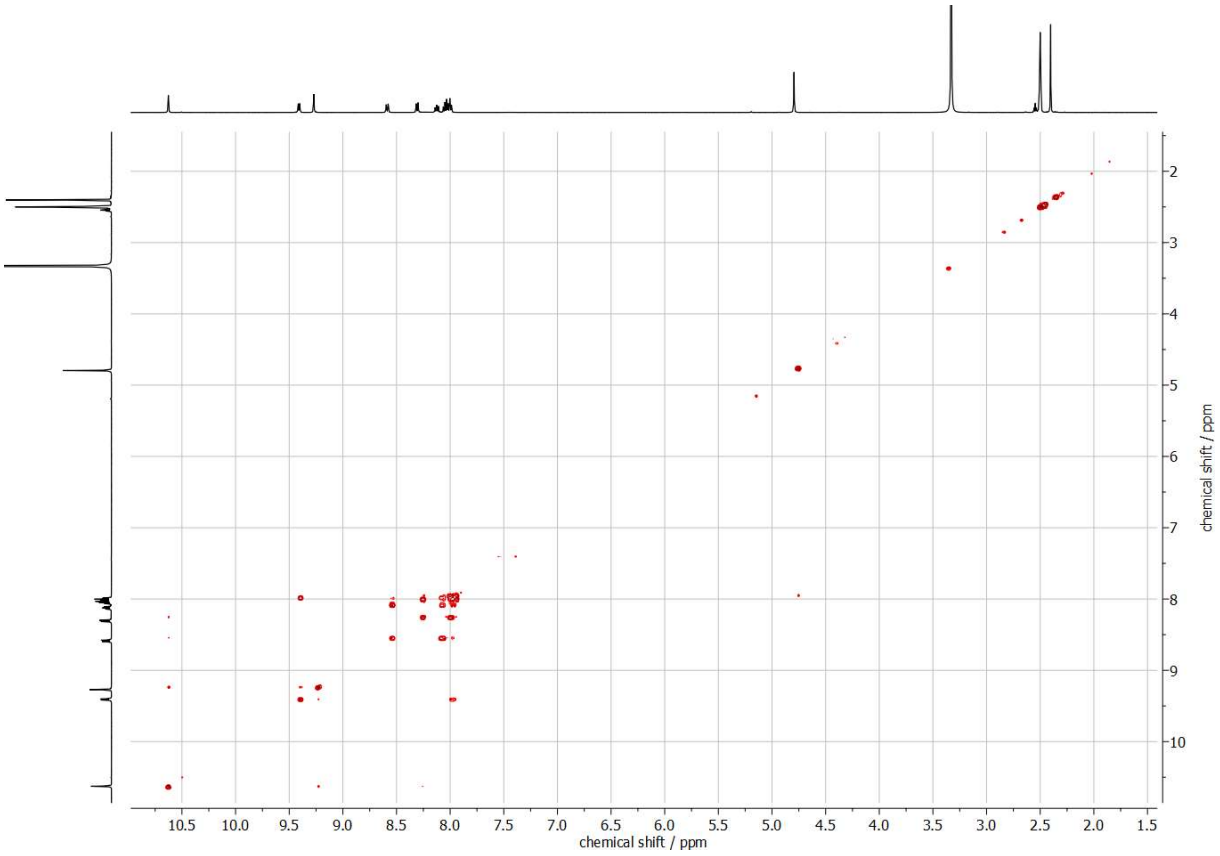

Figure S35. HH-COSY spectrum (500 MHz, DMSO-d_6, 25 °C) of **2b**.

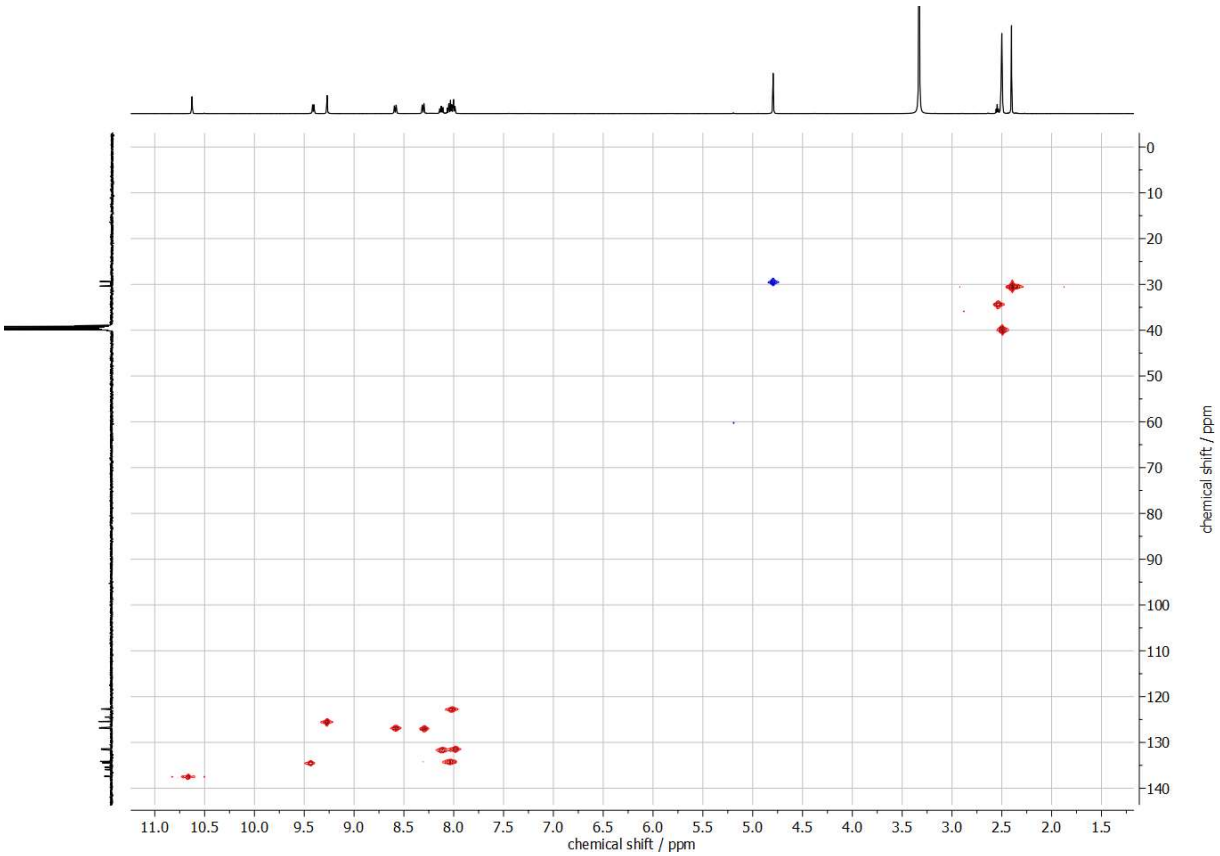

Figure S36. HSQC spectrum (500 MHz, DMSO-d_6, 25 °C) of **2b**.

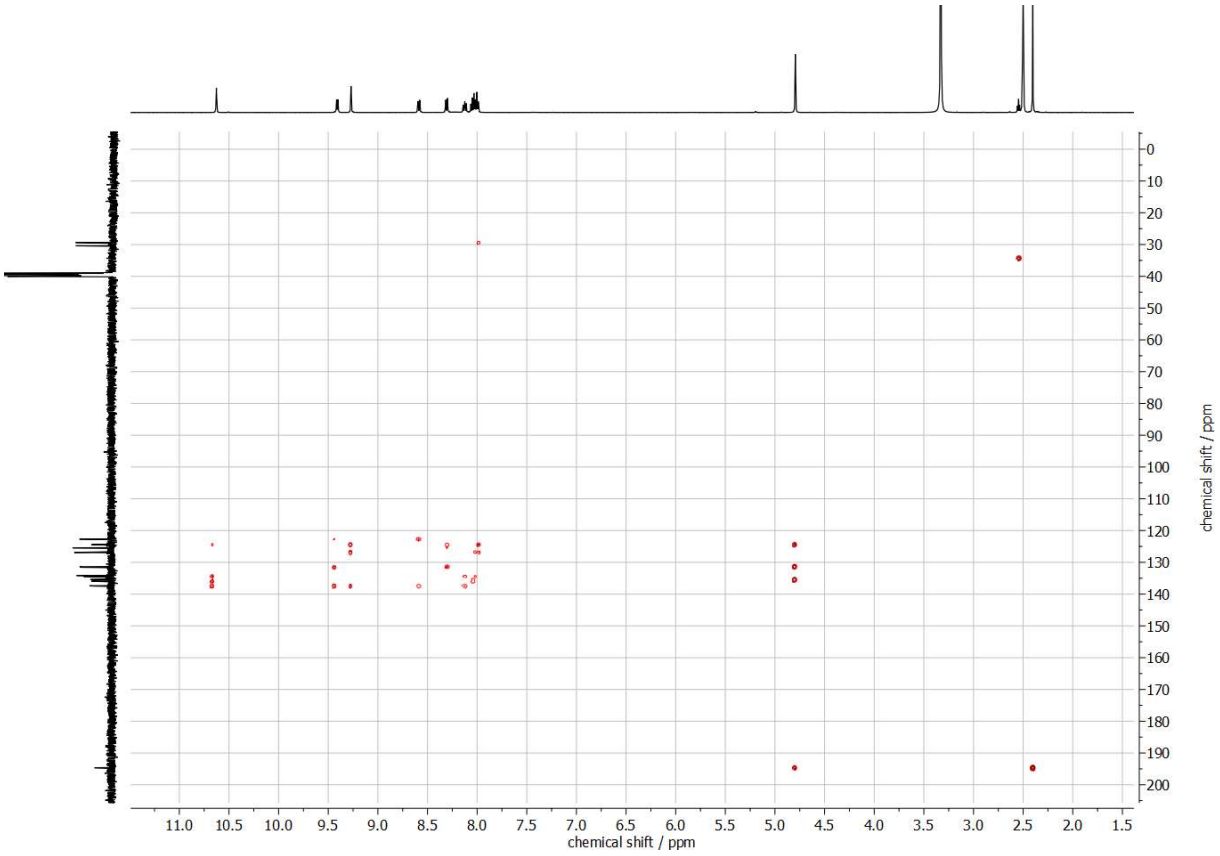

Figure S37. HMBC spectrum (500 MHz, DMSO-d_6, 25 °C) of **2b**.

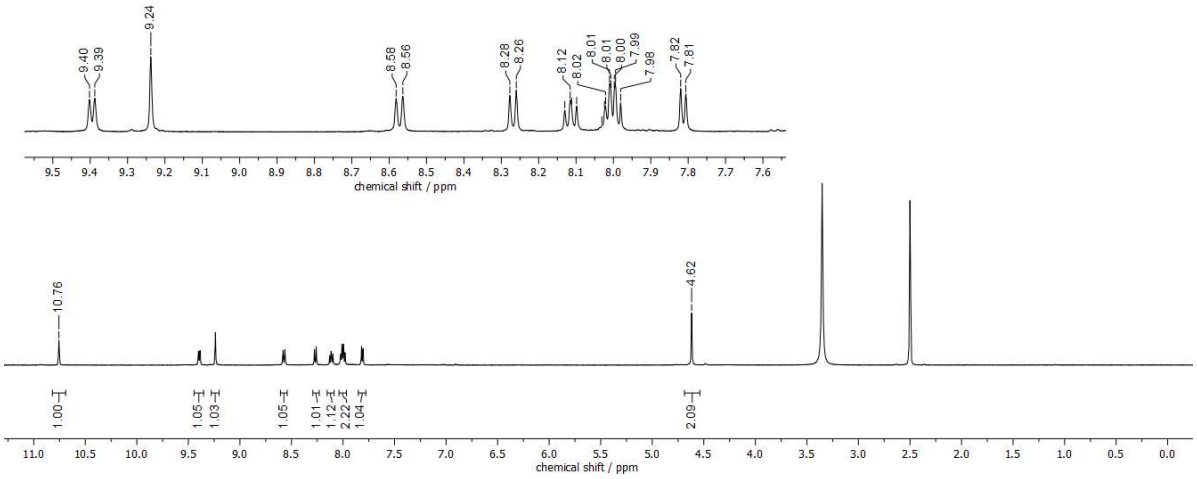

Figure S38. ^{1}H-NMR spectrum (500 MHz, DMSO-d_6, 25 °C) of **4b**.

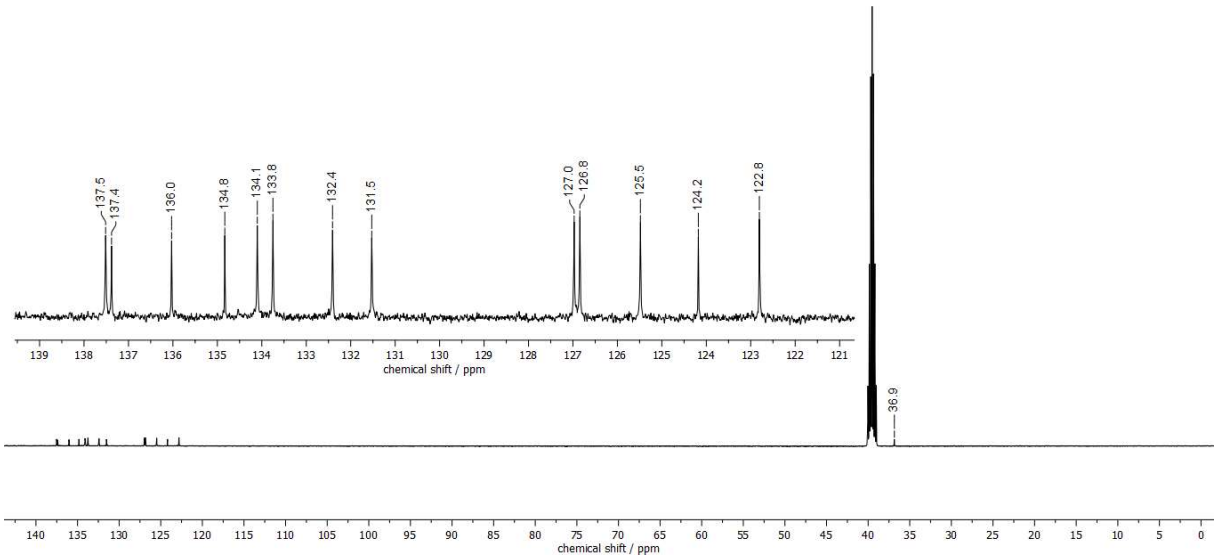

Figure S39. ^{13}C-NMR spectrum (500 MHz, DMSO-d_6, 25 °C) of **4b**.

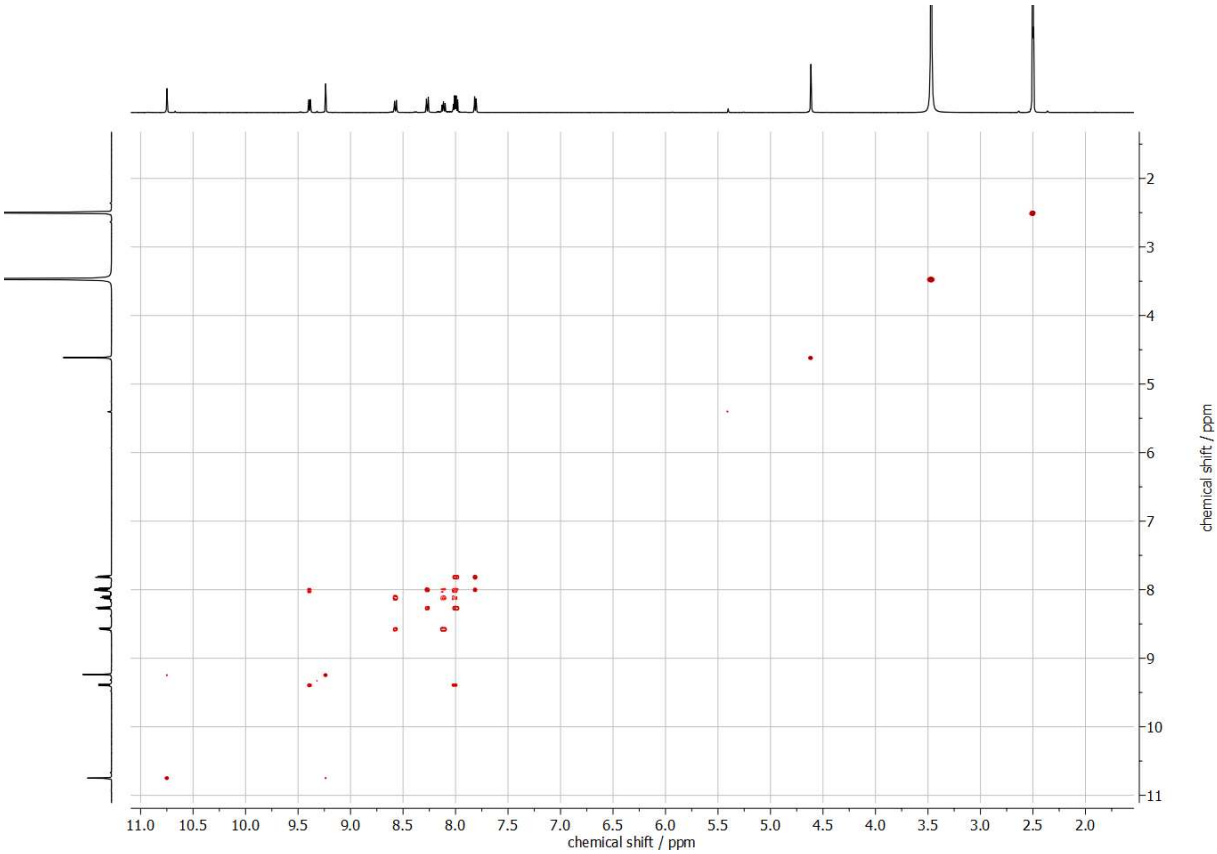

Figure S40. HH-COSY spectrum (500 MHz, DMSO-d_6, 25 °C) of **4b**.

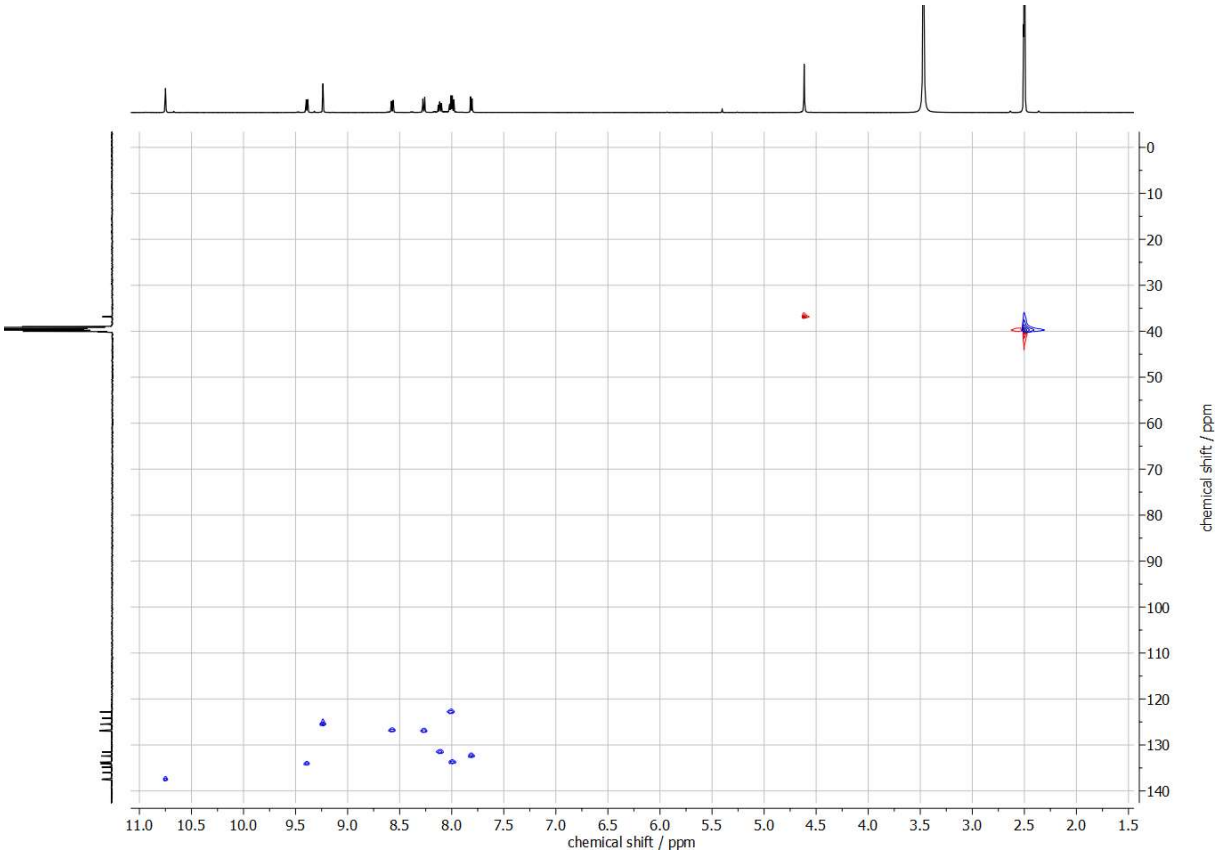

Figure S41. HSQC spectrum (500 MHz, DMSO-d_6, 25 °C) of **4b**.

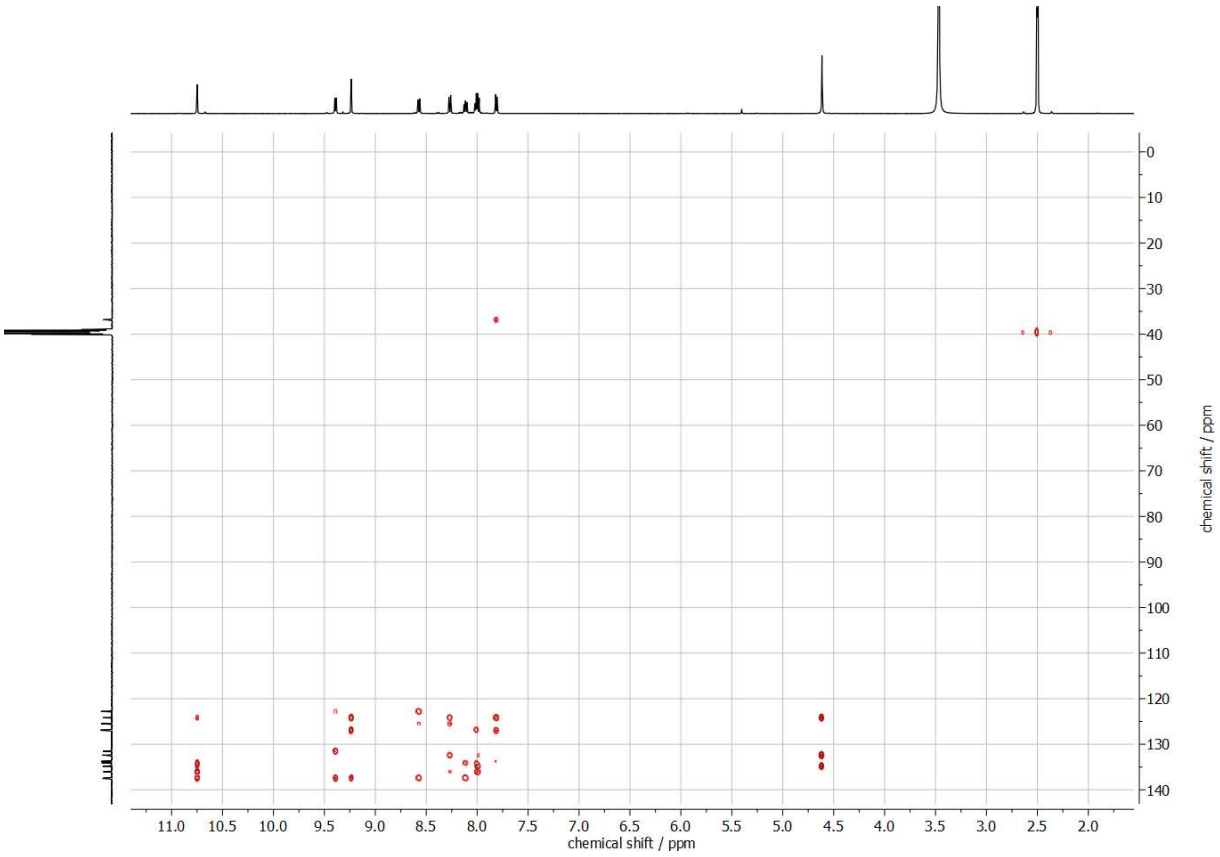

Figure S42. HMBC spectrum (500 MHz, DMSO-d_6, 25 °C) of **4b**.

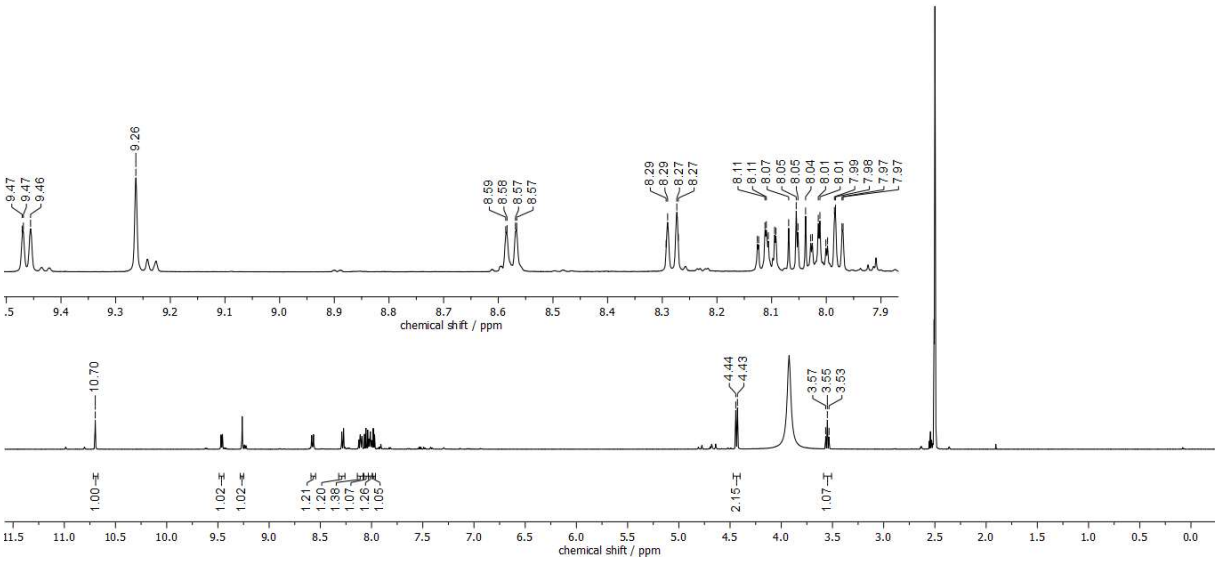

Figure S43. Crude ^{1}H-NMR spectrum (500 MHz, DMSO-d_6, 25 °C) of metastable **3b**.

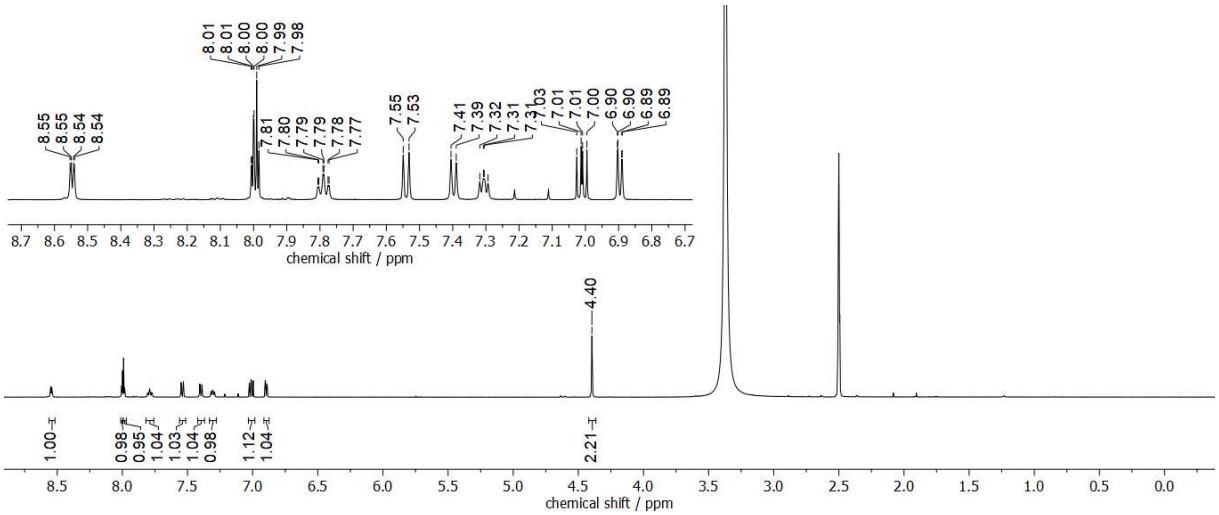

Figure S44. ^{1}H-NMR spectrum (500 MHz, DMSO-d_6, 25 °C) of **6–H$^+$**.

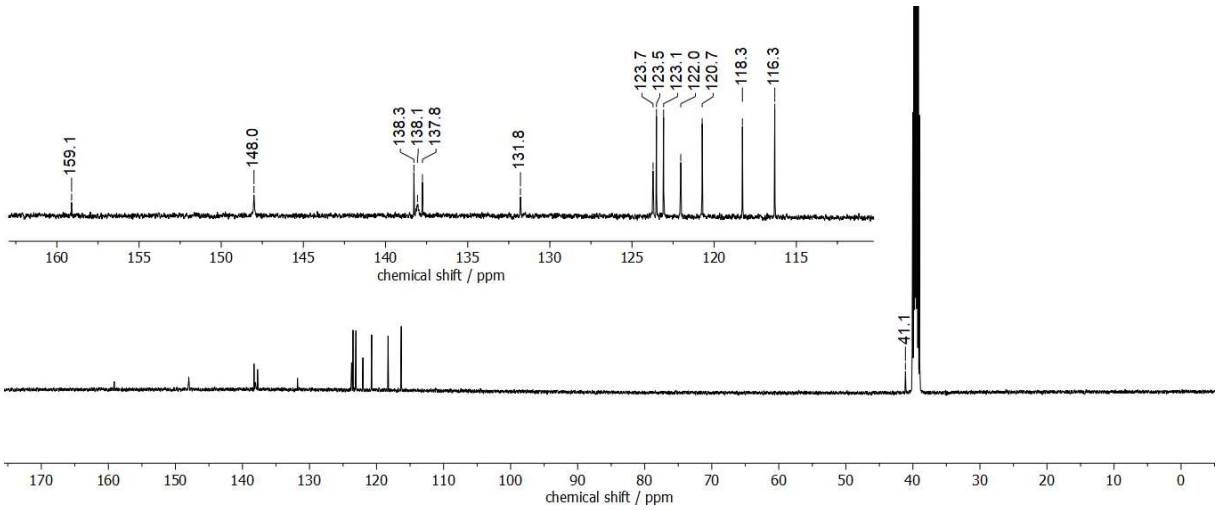

Figure S45. ^{13}C-NMR spectrum (125 MHz, DMSO-d_6, 25 °C) of **6–H$^+$**.

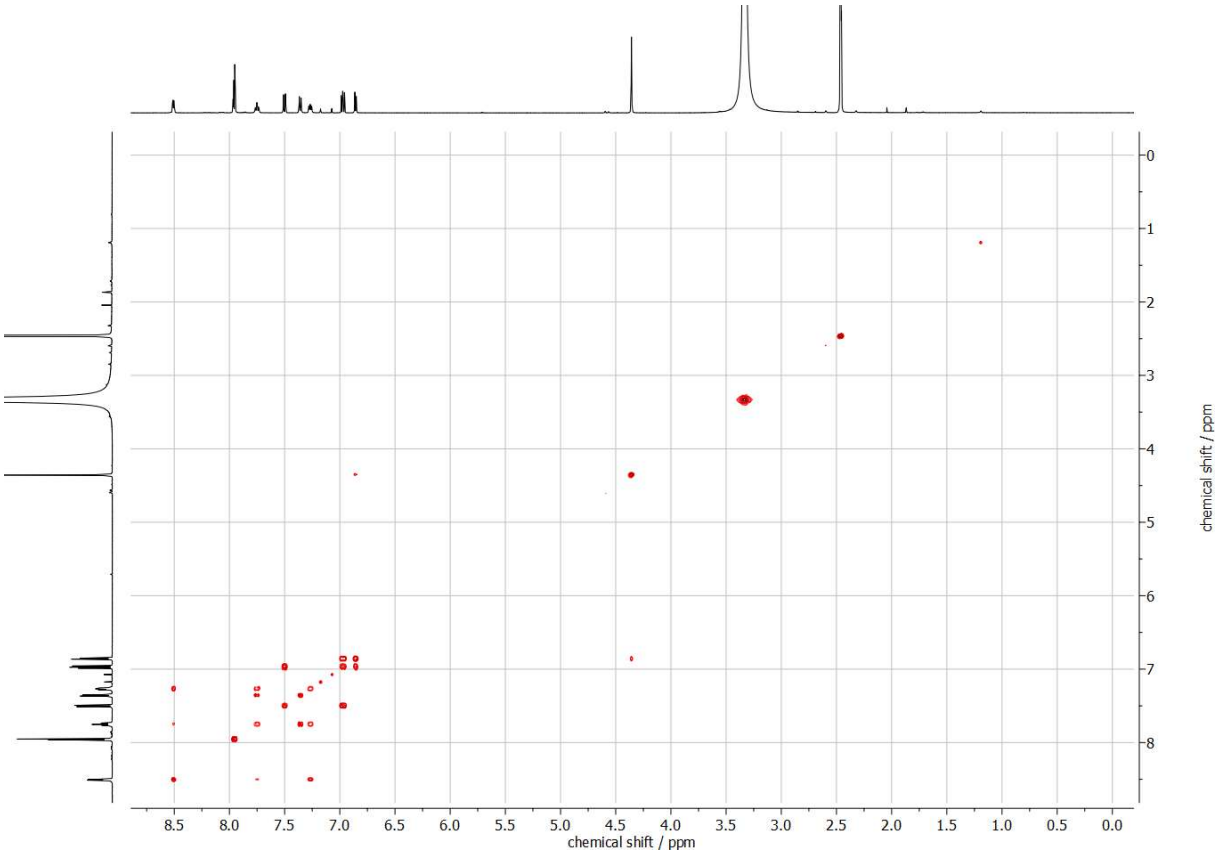

Figure S46. HH-COSY spectrum (500 MHz, DMSO-d_6, 25 °C) of **6–H$^+$**.

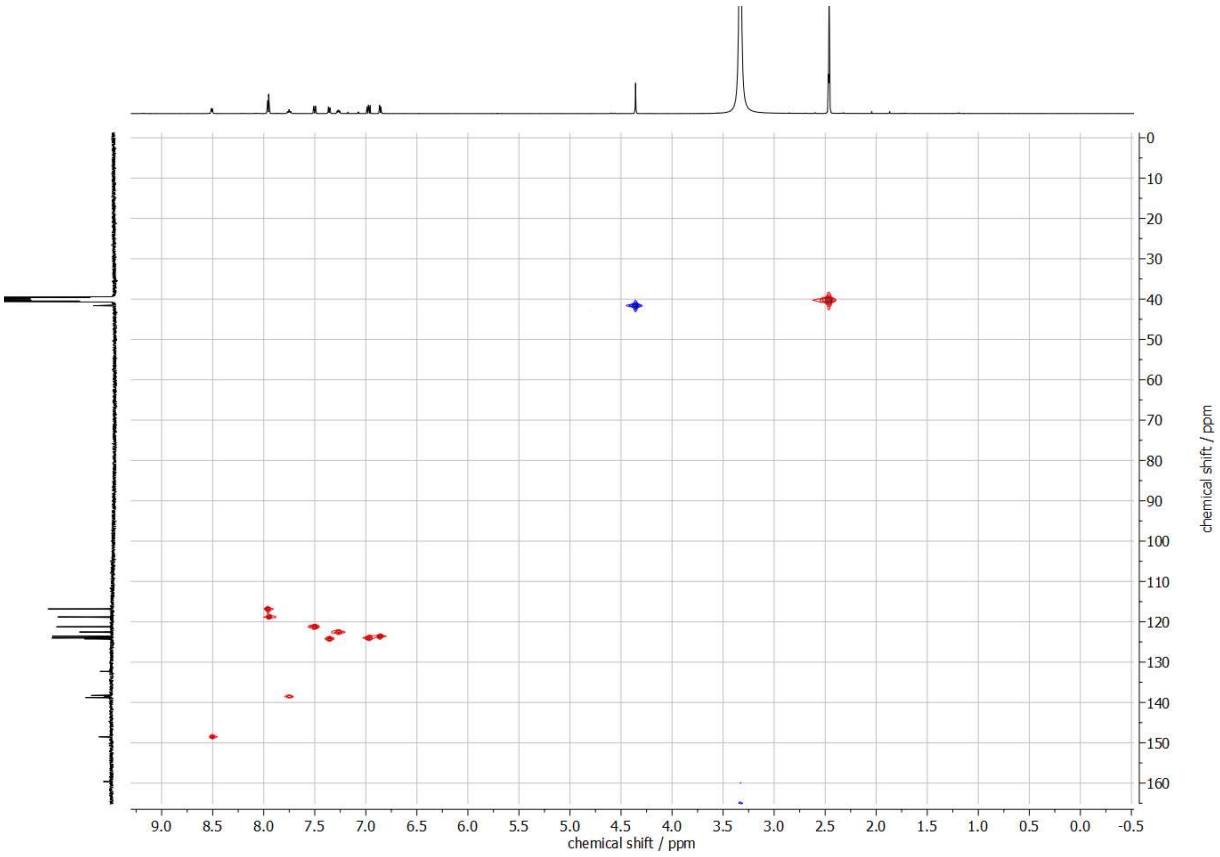

Figure S47. HSQC spectrum (500 MHz, DMSO-d_6, 25 °C) of **6–H$^+$**.

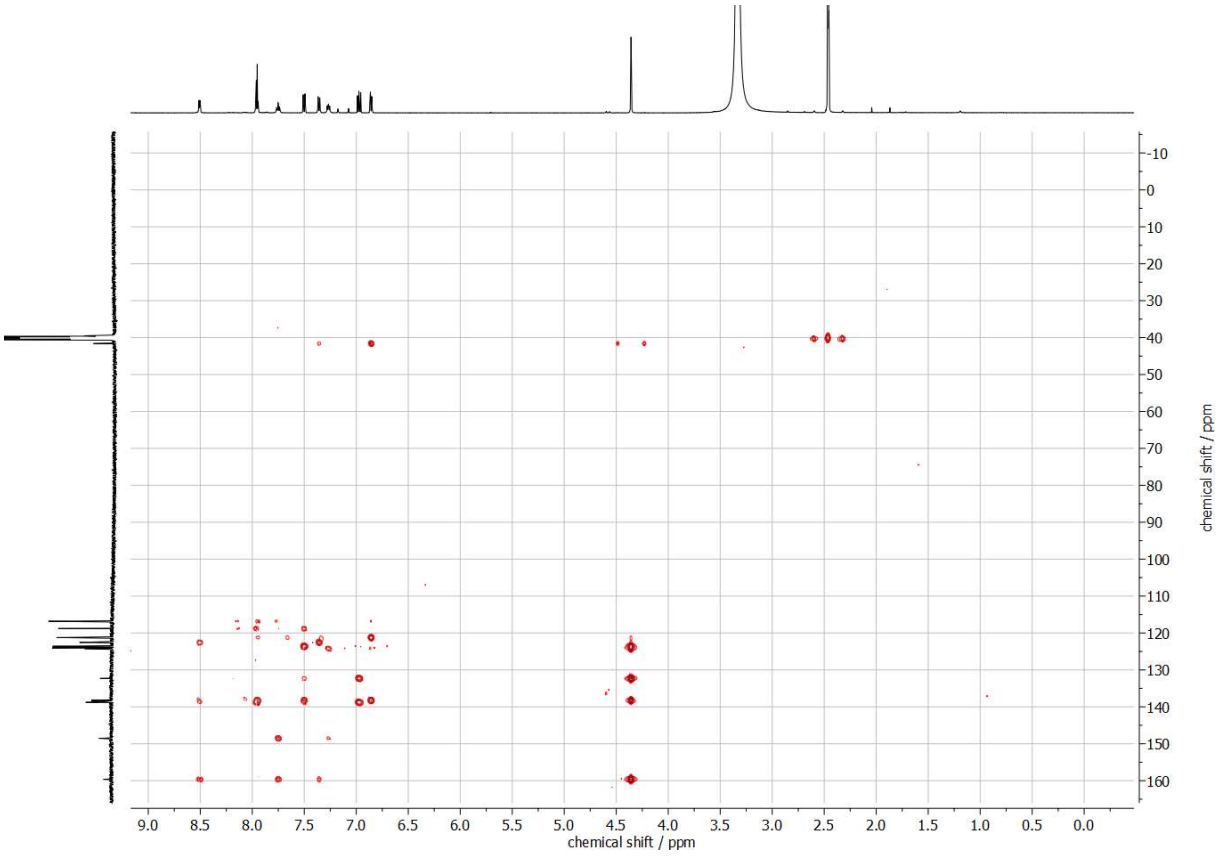

Figure S48. HMBC spectrum (500 MHz, DMSO-d_6, 25 °C) of **6–H$^+$**.

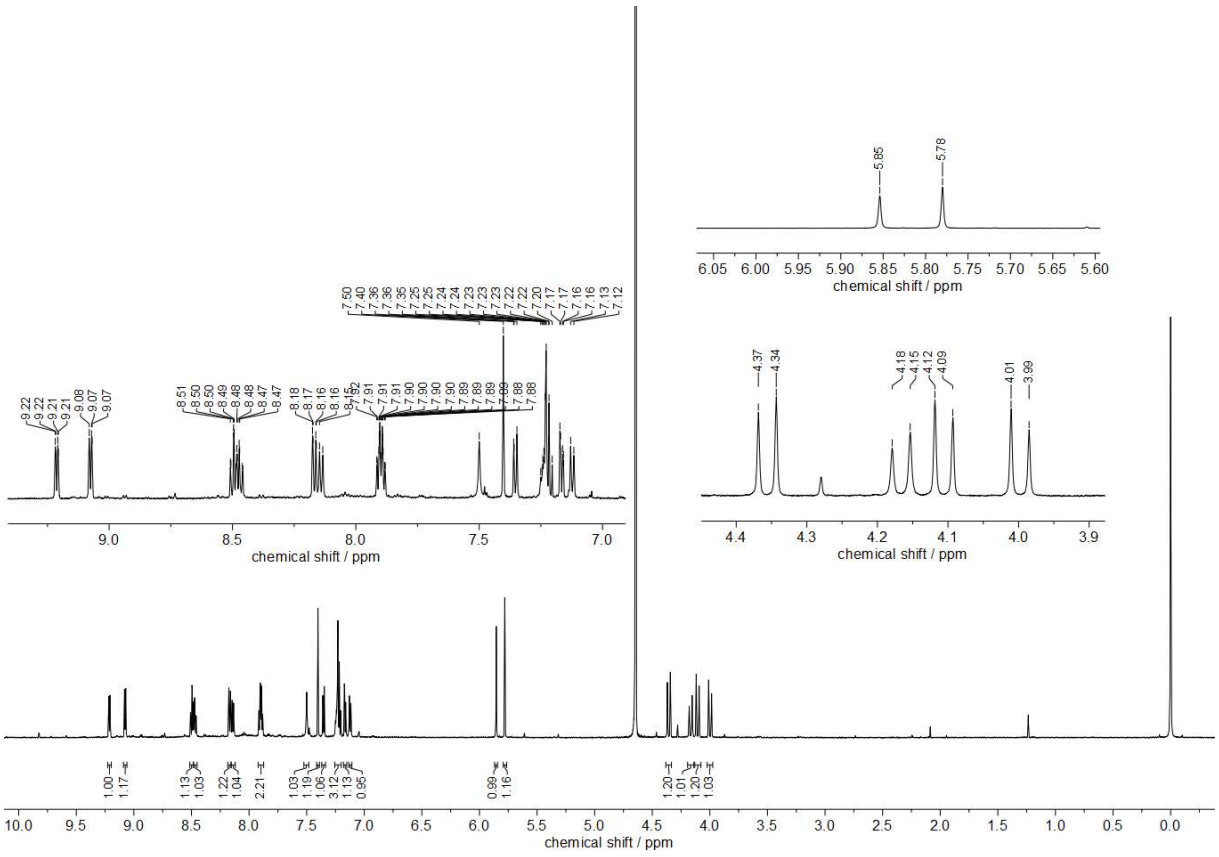

Figure S49. ^{1}H-NMR spectrum (600 MHz, D_2O, 40 °C) of the photolysate of **4b**.

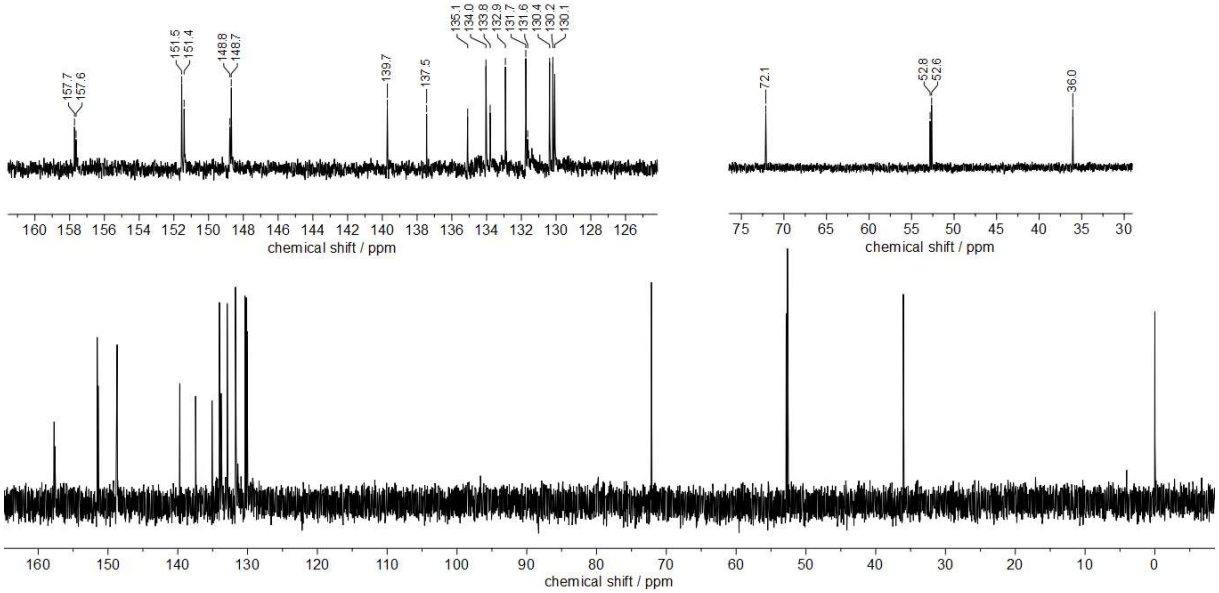

Figure S50. ^{13}C-NMR spectrum (125 MHz, D_2O, 40 °C) of the photolysate of **4b**.

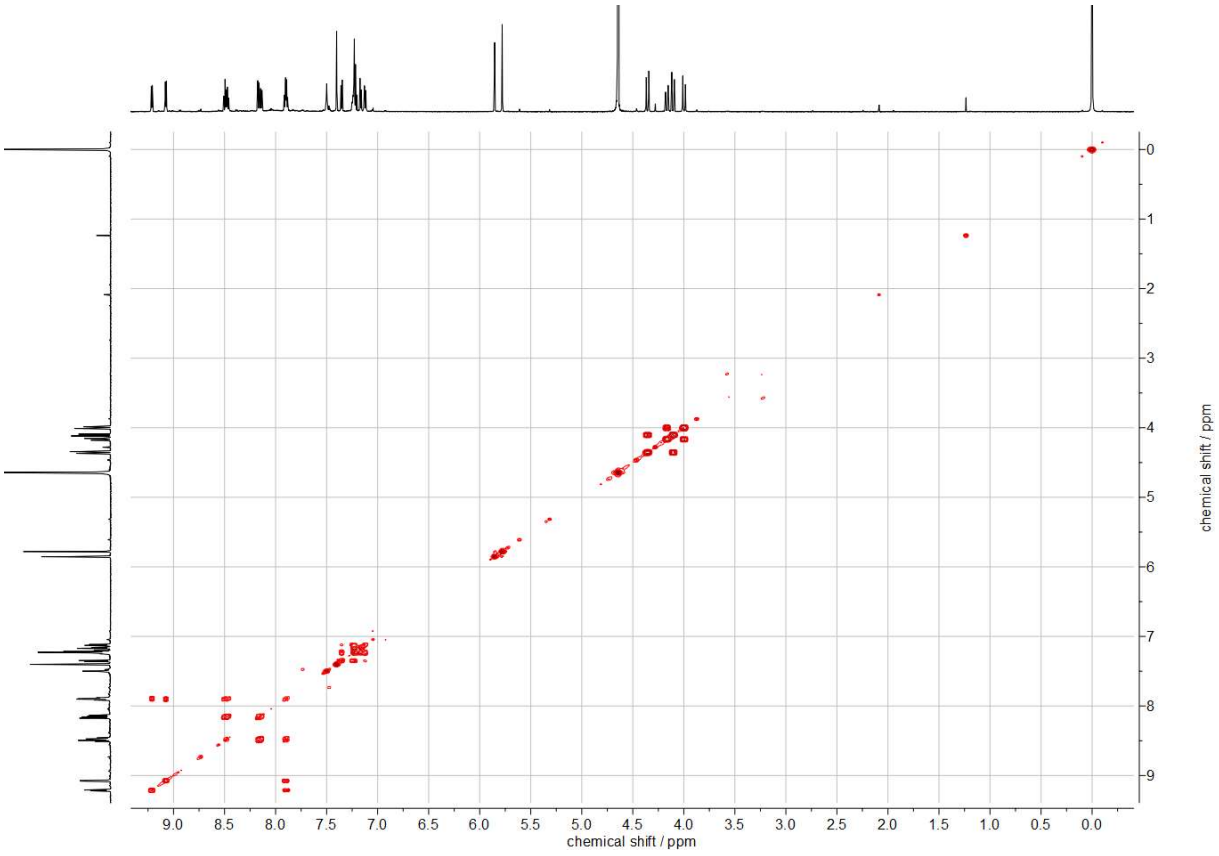

Figure S51. HH-COSY spectrum (600 MHz, D_2O, 40 °C) of the photolysate of **4b**.

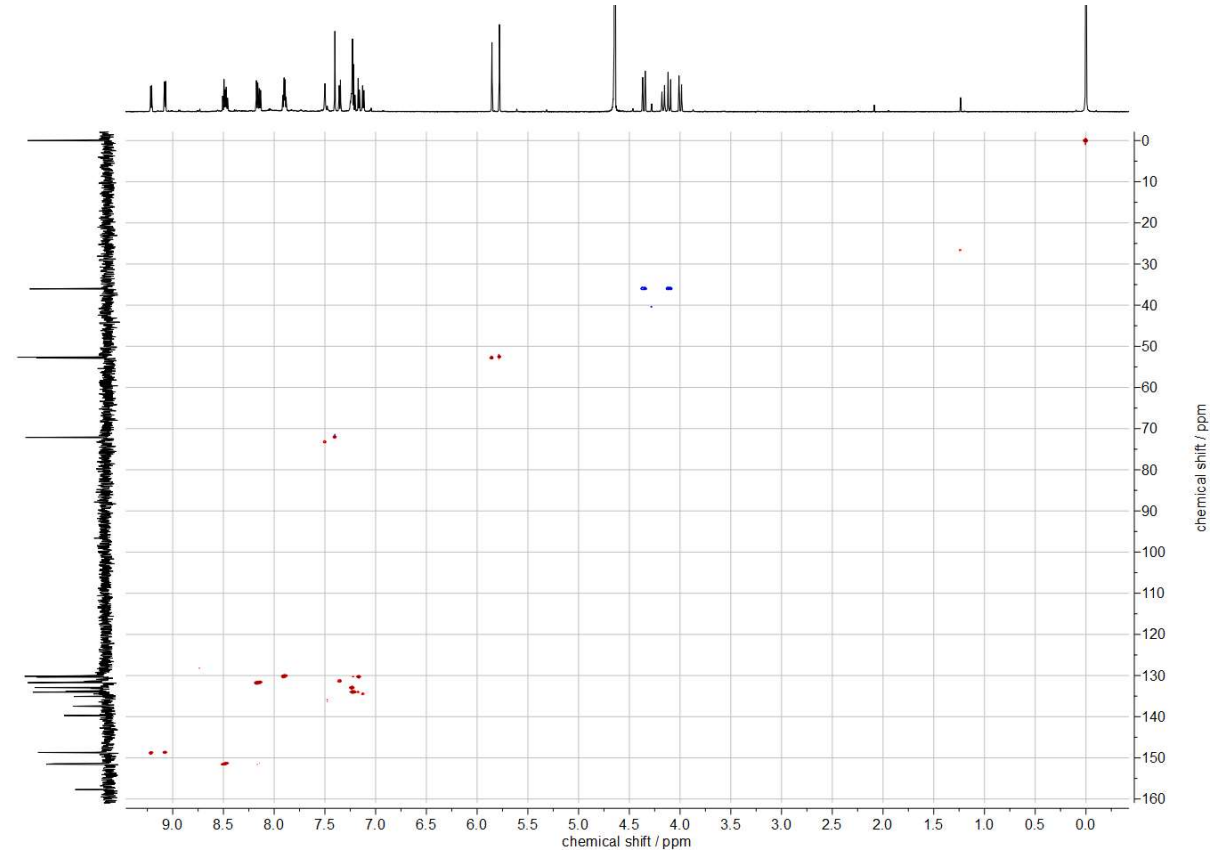

Figure S52. HSQC spectrum (600 MHz, D_2O, 40 °C) of the photolysate of **4b**.

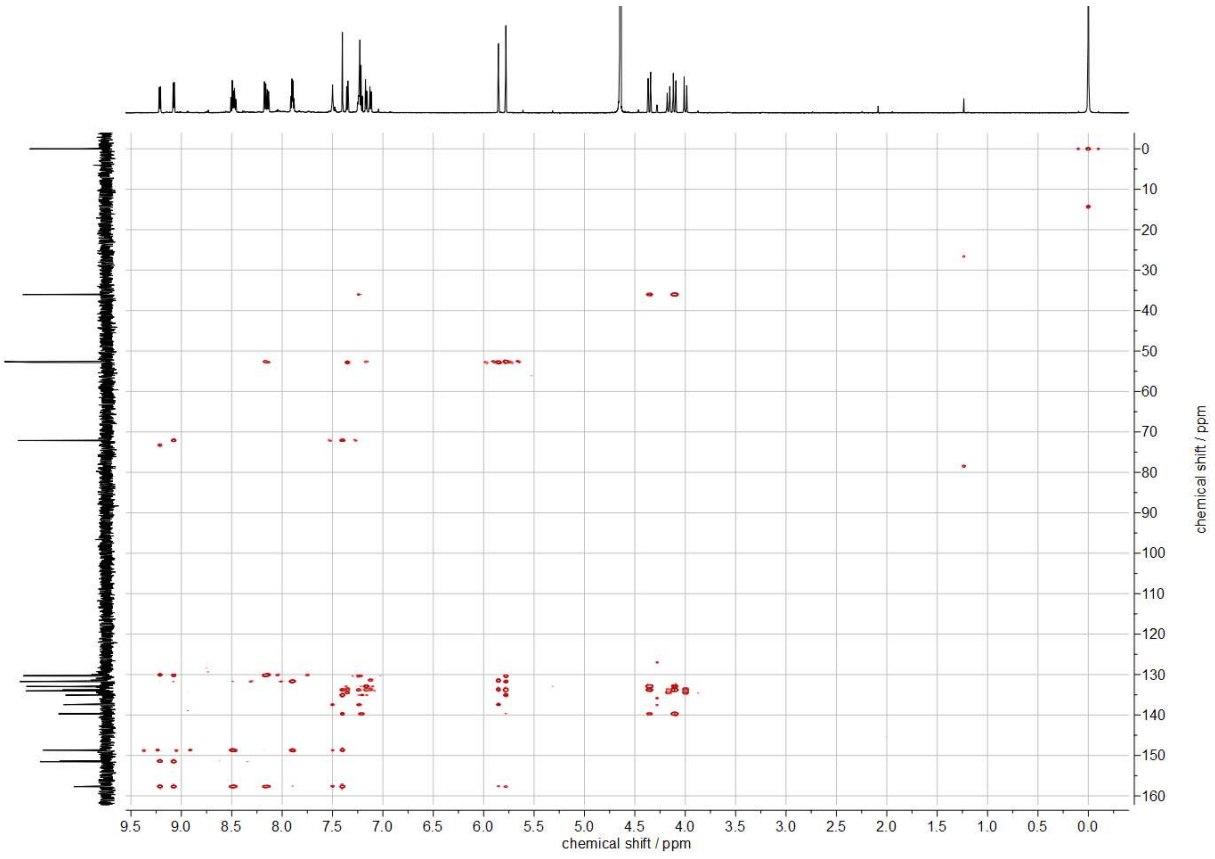

Figure S53. HMBC spectrum (125 MHz, D_2O, 40 °C) of the photolysate of **4b**.

7 Literatur

[1] K. Suzuki, A. Kobayashi, S. Kaneko, K. Takehira, T. Yoshihara, H. Ishida, Y. Shiina, S. Oishi and S. Tobita, *Phys. Chem. Chem. Phys.,* 2009, **11**, 9850.
[2] F. H. Stootman, D. M. Fisher, A. Rodger and J. R. Aldrich-Wright, *Analyst,* 2006, **131**, 1145.